Chlorophyll Can Be Reduced in Crop Canopies with Little Penalty to Photosynthesis[1][OPEN]

Berkley J. Walker,[a,b,c] Darren T. Drewry,[d,e] Rebecca A. Slattery,[a,b,f] Andy VanLoocke,[a,g] Young B. Cho,[a,b] and Donald R. Ort[a,b,f]*

[a]Global Change and Photosynthesis Research Unit, USDA/ARS, Urbana, Illinois 61801
[b]Carl R. Woese Institute for Genomic Biology, University of Illinois, Urbana, Illinois 61801
[c]Institute of Plant Biochemistry, Heinrich-Heine University, D-40225 Düsseldorf, Germany
[d]Jet Propulsion Laboratory, California Institute of Technology, Pasadena, California 91109
[e]Joint Institute for Regional Earth System Science and Engineering, University of California, Los Angeles, California 90095
[f]Department of Plant Biology, University of Illinois, Urbana, Illinois 61801
[g]Department of Agronomy, Iowa State University, Ames, Iowa 50011

ORCID IDs: 0000-0001-5932-6468 (B.J.W.); 0000-0002-7165-906X (R.A.B.); 0000-0002-5435-4387 (D.R.O.).

The hypothesis that reducing chlorophyll content (Chl) can increase canopy photosynthesis in soybeans was tested using an advanced model of canopy photosynthesis. The relationship among leaf Chl, leaf optical properties, and photosynthetic biochemical capacity was measured in 67 soybean (*Glycine max*) accessions showing large variation in leaf Chl. These relationships were integrated into a biophysical model of canopy-scale photosynthesis to simulate the intercanopy light environment and carbon assimilation capacity of canopies with wild type, a Chl-deficient mutant (*Y11y11*), and 67 other mutants spanning the extremes of Chl to quantify the impact of variation in leaf-level Chl on canopy-scale photosynthetic assimilation and identify possible opportunities for improving canopy photosynthesis through Chl reduction. These simulations demonstrate that canopy photosynthesis should not increase with Chl reduction due to increases in leaf reflectance and nonoptimal distribution of canopy nitrogen. However, similar rates of canopy photosynthesis can be maintained with a 9% savings in leaf nitrogen resulting from decreased Chl. Additionally, analysis of these simulations indicate that the inability of Chl reductions to increase photosynthesis arises primarily from the connection between Chl and leaf reflectance and secondarily from the mismatch between the vertical distribution of leaf nitrogen and the light absorption profile. These simulations suggest that future work should explore the possibility of using reduced Chl to improve canopy performance by adapting the distribution of the "saved" nitrogen within the canopy to take greater advantage of the more deeply penetrating light.

Global food production must increase to provide for the dietary needs of an increasing global population with greater affluence (Ray et al., 2013; Kromdijk and Long, 2016). One strategy to increase food production per unit land area is to increase the efficiency of photosynthetic conversion of photosynthetic photon flux density (PPFD; units noted in abbreviation table for this and subsequent abbreviations) into biomass, which is currently less than half the theoretical maximum in many major food crops (Long et al., 2015; Ort and Melis, 2015; Slattery and Ort, 2015). One reason for suboptimal conversion efficiency is that photosynthesis saturates above 25% of full sunlight and most incoming PPFD is absorbed by fully green upper canopy leaves, meaning that the majority of light absorption occurs where photosynthesis is least efficient due to saturation whereas lower layers have greater efficiency due to shading (Long et al., 2006; Zhu et al., 2008; Ort and Melis, 2011; Drewry et al., 2014). This situation suggests that decreasing leaf absorbance (L_A) through reductions in leaf chlorophyll content (Chl) could improve canopy assimilation efficiency by allowing more optimal distribution of PPFD within the canopy.

Increasing canopy photosynthesis through reduced Chl has been considered as a potential optimization strategy for over 30 years (as summarized in Laisk, 1982; Osborne and Raven, 1986). In an early modeling

[1] This research was supported via subcontract by the Bill and Melinda Gates Foundation (OPP1060461) titled "RIPE-Realizing Increased Photosynthetic Efficiency for Sustainable Increases in Crop Yield". D. Drewry was supported by the Jet Propulsion Laboratory, California Institute of Technology, under a contract with the National Aeronautics and Space Administration. B. Walker received support from the Alexander von Humboldt Foundation through a postdoctoral fellowship.

* Address correspondence to d-ort@illinois.edu. .

The author responsible for distribution of materials integral to the findings presented in this article in accordance with the policy described in the Instructions for Authors (www.plantphysiol.org) is: Donald R. Ort (d-ort@illinois.edu).

B.J.W., R.A.S., and D.R.O. conceived the idea of using light-green soybean germplasm to parameterize a canopy model; B.J.W. made the measurements of the light-green soybean optical properties and gas exchange parameters; Y.B.C. measured soybean protein content; B.J.W., D.T.D., and A.V. designed, performed, and interpreted the simulations; and B.J.W., D.T.D., R.A.S., A.V., and D.R.O. wrote the final paper.

[OPEN] Articles can be viewed without a subscription.

www.plantphysiol.org/cgi/doi/10.1104/pp.17.01401

approach integrating the simulated impact of Chl reduction of a single mutant accession to leaf and canopy light distribution to photosynthesis, Chl reduction was projected to increase soybean (*Glycine max* Merr.) canopy photosynthesis by 8% under clear-sky conditions, but much of this gain appears to be due to leaf-level improvements in light-saturated photosynthetic rates (Gutschick, 1984a, 1984b, 1988). Efforts to test the impact of reduced Chl on canopy-level carbon assimilation (A_{can}) have produced conflicting results. Although rates of carbon assimilation (A) of mutant algae with reduced light-harvesting capacity often show increased A when grown in mass culture (Melis, 1999; Polle et al., 2003; Mitra and Melis, 2008; Kirst et al., 2012), results from plant canopies are less clear perhaps because they represent complex arrangements of foliage through which radiation transfer processes and vertical variations in photosynthetic capacity interact (Leuning et al., 1995; De Pury and Farquhar, 1997; Baldocchi et al., 2002).

There is much experimental and computational work examining the possibility of increasing canopy photosynthesis through chlorophyll reduction on plant canopies on soybean (Gutschick, 1984a, 1984b, 1988; Pettigrew et al., 1989; Xu et al., 1994; Drewry et al., 2014; Slattery et al., 2016; 2017), which grows in dense canopies and has a large variety of accessions with reduced Chl (Supplemental Fig. S1; Fig. 1). One such accession is a magnesium chelatase mutant, *Y11y11* (Campbell et al., 2015), which contains less than half the Chl on a leaf area basis of its nearly isogenic wild type. Some experiments with *Y11y11* show an increase in A_{can} (Pettigrew et al., 1989) and others show little or no effect (Xu et al., 1994; Slattery et al., 2017) despite more even leaf-level light distribution to chloroplasts (Slattery et al., 2016). In the most systematic field examinations to date, leaf rates of carbon assimilation (A_{leaf}), A_{can}, conversion efficiency of absorbed PPFD into biomass, and yield were compared between the *Y11y11* and the nearly isogenic wild type. Although there were no clear benefits to canopy-level carbon assimilation, there was also little detriment. Despite a greater than 50% reduction in Chl, only modest reductions in biomass and yield were observed likely due to the negative pleiotropic effects specific to *Y11y11*, discussed below (Slattery et al., 2017).

The conflicting results concerning the benefits of Chl reduction in higher plant canopies may partially result from the limitations of fieldwork where environment is variable and a limited number of accessions can be examined simultaneously. Given the complex interactions of dense plant canopies with incoming PPFD (i.e. Drewry et al., 2010a, Niinemets, 2007; Hikosaka et al., 2016), it is possible that a selected cultivar with reduced Chl has leaf optical properties that are sub- or supra-optimal for a given season depending on environmental forcing and plant development for that particular year. In addition, negative pleiotropic effects can accompany light-green phenotypes due to the specific nature of the mutation, further confounding experimental results. For example, environmental differences combined with pleiotropic effects might explain the conflicting differences measured in *Y11y11*, which has higher water loss due to increased stomatal conductance. In water-replete conditions, *Y11y11* had higher A_{can} as compared to wild type (Pettigrew et al., 1989), whereas no difference was observed under water-limiting conditions (Slattery et al., 2017).

Because A measurements are often localized temporally or spatially to a few positions in the canopy, a vertically resolved modeling approach that incorporates the detailed biophysical coupling among radiation transfer, photosynthetic biochemical capacity, and canopy development can provide insights into the complex relationship between leaf Chl and A_{can}. Here we use a multilayer canopy-root-soil model (MLCan), which couples the biophysical, ecophysiological, and biochemical functions of above-ground vegetation with a vertically resolved model of soil moisture to simulate and directly evaluate the impacts of leaf Chl and associated optical properties in canopies that are otherwise identical (Drewry et al., 2010a, 2010b). MLCan is driven by meteorological data and integrates vertically resolved leaf-level exchanges of CO_2, water vapor, and energy to canopy-scale fluxes. Such canopy models use assumptions of leaf optical properties [leaf reflectance (L_R), leaf transmittance (L_T), and leaf absorbance (L_A)] to simulate within-canopy distributions of PPFD as functions of downwelling solar radiation, solar zenith angle, foliage density, and leaf angle distributions (De Pury and Farquhar, 1997; Campbell and Norman, 1998; Lai et al., 2000; Baldocchi et al., 2002; Drewry et al., 2010a).

An additional consideration of the ability of Chl reduction to increase canopy photosynthesis is the impact of subsequent redistribution of N and photosynthetic capacity. Chlorophyll is associated with a large portion of leaf nitrogen, not only present in the Chlorophyll (four molecules to complex the magnesium ion or 0.06 g N mmol Chl^{-1}), but also in the Photosystem I and II core complexes (PSI and PSII, respectively), and the light harvesting complexes that coordinate the chlorophyll molecules for light energy capture. The chlorophyll binding proteins of the light reactions and antenna complex contain 5000, 6040, and 338 mol N (mol reaction center or LHCII molecule)$^{-1}$ for PSII, PSI, and LHCII, respectively (Hikosaka and Terashima, 1995). Assuming that PSII, PSI, and LHCII are associated with 60, 184, and 13 chlorophyll molecules each, this means that the total nitrogen associated with each chlorophyll molecule is 1.23, 0.52, and 0.42 g N mmol Chl^{-1} for chlorophyll associated with PSII, PSI, and LHCII respectively (Evans and Seemann, 1989; Kühlbrandt et al., 1994; Hikosaka and Terashima, 1995; Niinemets and Tenhunen, 1997). In soybean, chlorophyll-related N is not trivial; for example, fully expanded field-grown soybean leaves contained 1.75 g N m^{-2} and Chl of 320 μmol m^{-2} (Ainsworth et al., 2007), resulting in a total chlorophyll-associated N cost of 8% to 22% depending on how much chlorophyll is

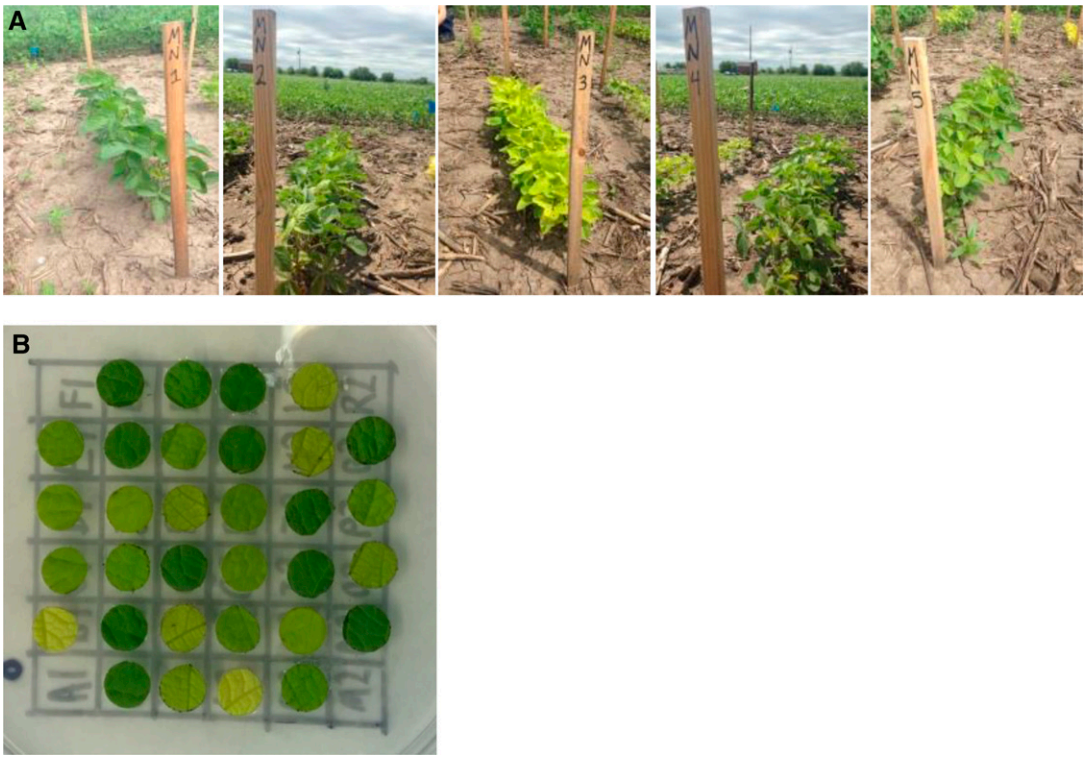

Figure 1. Examples of some of the 67 soybean lines with decreased chlorophyll content (A). Leaf punches prepared for chlorophyll fluorescence imaging (B). Most of the lines were obtained from the USDA soybean germplasm collection and others from the Fast Neutron Soybean Mutagenesis project. Lines were characterized for chlorophyll content, leaf transmittance, and leaf reflectance.

partitioned to each chlorophyll binding protein. This nitrogen must be partitioned through the canopy, and theoretical analyses have suggested that the vertical distribution of leaf nitrogen should optimally be in direct proportion to light intensity at a given canopy layer (Field, 1983; Leuning et al., 1995; Sands, 1995), but experimental evidence demonstrates that canopies do not optimally distribute nitrogen, instead overinvesting nitrogen when irradiance is low and underinvesting when irradiances are high (Niinemets, 2007, 2015). These observations suggest two hypotheses that can be tested: 1) there is a significant N investment in Chl-related proteins that can be decreased through Chl reduction with minimal impact to canopy photosynthesis; and 2) changes in Chl impact canopy PPFD distribution enough to change optimal vertical nitrogen distribution.

Here we parameterize MLCan with the field measured relationships among Chl, leaf optical properties, and leaf biochemistry to more realistically simulate the integrated canopy response to Chl reduction, as well as resolve leaf-level variations that could translate to changes in A_{can} and determine the metabolic savings (in terms of actual chlorophyll molecules and associated proteins) of canopies with reduced leaf absorbance (L_A). In one set of simulations, this revised MLCan model was parameterized with leaf properties of a wild type (*cv* Clark) and the nearly isogenic low-Chl *Y11y11* mutant (Pettigrew et al., 1989; Campbell et al., 2015; Slattery et al., 2017). In a second set of simulations, we simulated synthetic canopies constructed with foliage across a range of Chl that indicate Chl can be reduced by up to 80% with only slight decreases in A_{can}. Additionally, whereas Chl reduction can often result in vertically resolved canopy domains with higher light use efficiencies, these increased efficiencies only resulted in higher net A in the lower canopy layers of dense canopies and did not result in a net canopy improvement to carbon fixation capacity. Furthermore, although lower Chl canopies were expected to have different optimal nitrogen distributions, changes in N distribution through the canopy alone were not found to increase A_{can} as compared to dark-green canopies. These findings present valuable quantitative relationships among Chl, leaf optical properties, and biochemistry for future efforts in optimizing canopy performance through Chl reduction, and more broadly for modeling the impact of Chl variation on canopy biophysics.

RESULTS

We present the results of the empirical measurements and numerous canopy simulations in three main subsections to better organize their content and motivation.

The first subsection ("Empirical Relationships among Leaf Optical Properties, Photosynthetic Biochemistry, and Chl") presents the primary empirical relationships among leaf optical properties, photosynthetic biochemistry, and Chl measured across the panel of field-grown soybean accessions displaying a range of Chl that were used to parameterize subsequent canopy simulations in the second and third subsections ("Comparisons between a Simulated Wild-Type and *Y11y11* Canopy" and "Using Synthetic Canopies To Explore a Range of Chl and Nitrogen Distributions"). The second subsection ("Comparisons between a Simulated Wild-Type and *Y11y11* Canopy") tests if a specific accession (*Y11y11*) is expected to show an increased canopy and/or within-canopy performance through detailed daily and season-long comparisons between a simulated canopy of wild-type and *Y11y11* soybeans. This accession was selected due to the amount of available field data to provide parameterizations and model validation. The third subsection ("Using Synthetic Canopies to Explore a Range of Chl and N Distributions") determines, by simulating synthetic canopies with a broad range of Chl amounts, if there is any change in leaf Chl level that would be predicted to increase photosynthetic performance. The impact of biochemical capacity scaling with Chl is explored in the simulations of "Empirical Relationships among Leaf Optical Properties, Photosynthetic Biochemistry, and Chl" and "Comparisons between a Simulated Wild-Type and Y11y11 Canopy" by either including or not the relationship measured and presented in "Empirical Relationships among Leaf Optical Properties, Photosynthetic Biochemistry, and Chl". Additionally, the impact of changing nitrogen distribution, and subsequent vertical biochemical capacity distribution, is investigated in both sets of simulations.

Empirical Relationships among Leaf Optical Properties, Photosynthetic Biochemistry, and Chl

A panel of 67 Chl deficient mutants and parent lines provided an approximately uniform distribution of Chl across the range of approximately 100 μmol m^{-2} to 500 μmol m^{-2} resulting in a similarly wide range of leaf optical properties (Fig. 2). As expected, L_R and L_R decreased with increasing Chl whereas L_A increased with increasing Chl (Fig. 2). Interestingly, although the ratio of L_R to L_R showed no clear trend as a function of Chl (Supplemental Fig. S1A), the average value across all accessions was approximately 1 across most of the photosynthetically active radiation (PAR) spectrum (Supplemental Fig. S1B). The relationships between Chl and leaf optical properties for the PAR region of the spectrum from the data are shown in Figure 2 (see Eqs. 1 and 2; and see final fits in Supplemental Fig. S3).

There was a clear relationship between Chl and both V_{cmax} and J_{max} in our accessions with reduced Chl (Fig. 3; Eqs. 3 and 4). There was also a strong

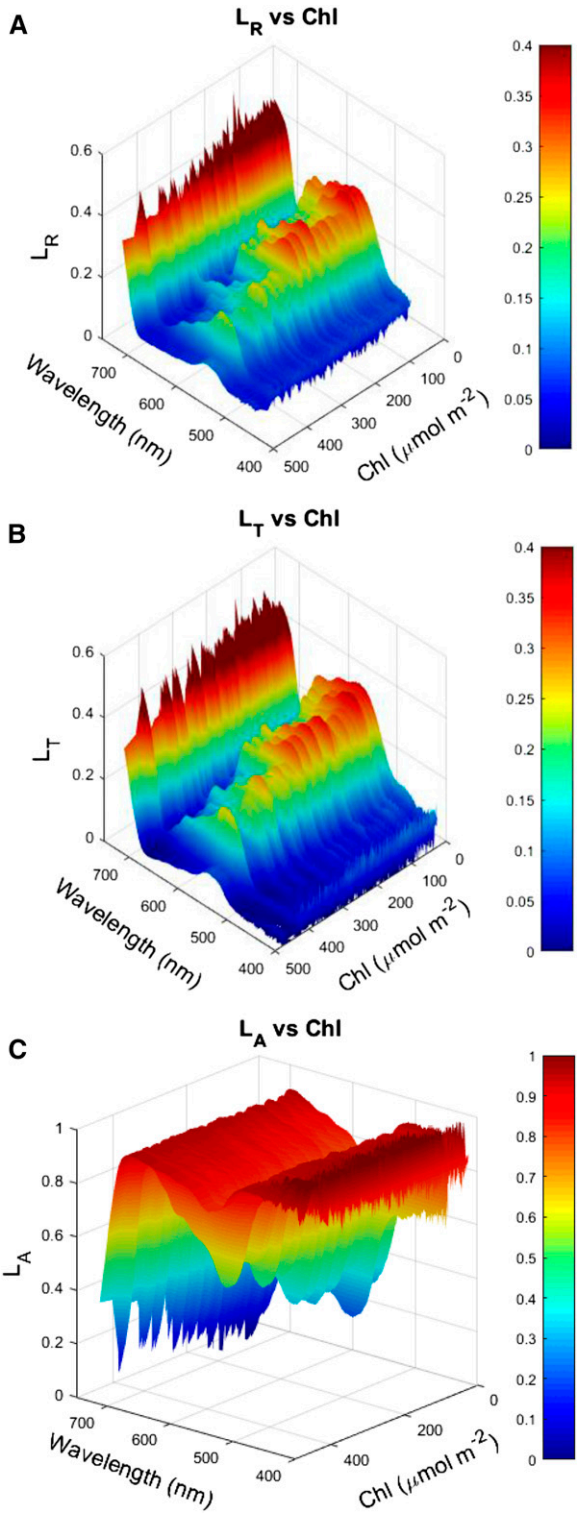

Figure 2. Shown are the relationships between leaf chlorophyll content and reflectance (L_R, A), transmittance (L_T, B), and absorbance (L_A, C) across the spectrum of photosynthetically active radiation.

relationship between Chl and total carotenoids (R^2 = 0.75; Supplemental Fig. S2). This relationship was linear for much of the Chl range with between 0.3 and 0.4

carotenoid molecules per chlorophyll molecule but increased at low Chl until there were more carotenoid molecules than chlorophyll molecules (Supplemental Fig. 2B).

Notably, there was variability in the relationship between V_{cmax} and Chl, indicating some cultivars maintained higher V_{cmax} for a given Chl than others, and pointing to the potential for the development of plants with low Chl and high photosynthetic biochemical capacity. Consistent with past work, which saw no significant differences in the V_{cmax} or J_{max} of *Y11y11* compared to the wild type (Slattery et al., 2017), we saw only slight differences in the V_{cmax} or J_{max} of *Y11y11* as compared to the higher Chl lines (Fig. 3). A similar increase in variability across the mean was observed in J_{max} as Chl decreased below approximately 250 μmol m^{-2} (R^2 of 0.21). This decrease in J_{max} could have been driven in part by lower photosystem II (PSII) quantum efficiency in some mutant lines with reduced Chl. Indeed, chlorophyll fluorescence analysis revealed that the maximum efficiency that PSII was able to use photons to perform photochemistry (F_v/F_m), and electron transport rates showed similar increasing variability in these parameters in lines with reduced Chl (Supplemental Fig. S4; Baker, 2008). There was no clear correlation between Chl and stomatal conductance (g_s) or leaf day respiration (R_d; Supplemental Fig. S5).

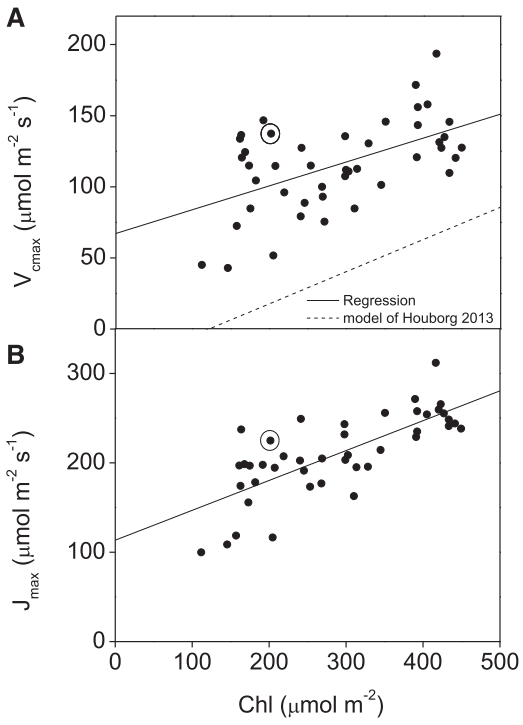

Figure 3. a, b, Observed impact of the variation in Chl content on photosynthetic performance. Forty-five plants from various cultivars of soybean were measured using a 6400-XT gas exchange system (LI-COR) to derive maximum rate of carboxylation (V_{cmax}) and electron transport (J_{max}) from photosynthetic carbon dioxide response curves. Chl was determined from SPAD (Soil Plant Analysis Development) measurements according to the relationship presented in Supplemental Fig. S12. Also shown is the modeled relationship of Chl to V_{cmax} of Houborg et al. (2013; dotted line). Circled data represents the values measured in the low chlorophyll mutant *Y11y11*.

Comparisons between a Simulated Wild-Type and *Y11y11* Canopy

The relationships measured above were next incorporated into daily and seasonal simulations of wild-type and *Y11y11* soybean canopies to investigate the PPFD and *A* distribution of this well-studied accession. Seasonal incident PPFD, air temperature, precipitation, and ambient water vapor pressure were identical between the wild-type and *Y11y11* simulations whereas seasonal variations in leaf area index (LAI) and Chl were constructed from interpolated measurements from the 2013 growing season (Supplemental Fig. S6; Slattery et al., 2017). As shown previously, the seasonal LAI was similar between wild type and *Y11y11* (Supplemental Fig. 6E), but the leaf area distribution (LAD) of *Y11y11* was denser in the lower canopy (Slattery et al., 2017). Leaf optical properties were varied over the growing season according to leaf Chl using the empirically measured relationship for each cultivar (Fig. 2, Supplemental Fig. S3; Eqs. 1 and 2). Additionally, although not incorporated into MLCan but important for understanding N use efficiency and partitioning, neither leaf nitrogen nor soluble protein content were different between wild type and *Y11y11* for most sampled days, the exception being a significantly higher soluble protein content on a leaf area and weight basis on days of the year (DOY 193; Supplemental Fig. S7). Interestingly, because *Y11y11* had approximately half the Chl as wild type, and leaf nitrogen and soluble protein were similar, this resulted in a lower percentage of leaf nitrogen associated with Chl, assuming all Chl was bound by LHCII, the lowest nitrogen containing chlorophyll binding protein (0.42 g nitrogen mmol Chl^{-1}) and a higher protein/Chl ratio in *Y11y11* (Supplemental Fig. S7).

Daily Simulations of Wild-Type and Y11y11 *Soybean with Accession-Specific Parameterizations*

To examine the temporally and spatially resolved impacts of variations in chlorophyll content and associated leaf optical properties of field-grown *Y11y11*, simulations were conducted for two representative DOYs (193 and 230) with similar total downwelling PPFD but distinguished by canopy LAI (early and late growing season). These simulations allowed us to visualize the differences in the radiative regime and vegetation function that were induced by the contrasting properties of wild-type and *Y11y11* plants, both throughout the vertical canopy space and over the course of diurnal variation in environmental forcing

(Fig. 4). Early in the season when LAI was low (approximately 2.7), wild-type canopies had only slightly greater PPFD absorbance ($PPFD_A$) than their light-green counterparts in the upper approximately 40% of the canopy, which drove greater A at upper layers within the canopy in wild type (Fig. 4, A and C). Later in the season when the canopies were more dense, wild-type canopies had greater $PPFD_A$ in the upper approximately 10% to 20% of the canopy, whereas *Y11y11* $PPFD_A$ was greater in the lower 75% to 80% (Fig. 4B). These differences in $PPFD_A$ distribution in denser canopies drove different rates of A throughout the vertical canopy domain, with wild-type plants having greater A in the top 10% of the canopy at midday and *Y11y11* having higher A in the lower 90% of the canopy relative to wild-type plants (Fig. 4D). On both days, *Y11y11* canopies generally had a higher quantum efficiency (Φ_{CO2}) in most canopy layers, indicating more efficient use of $PPFD_A$ due to less oversaturation of photosynthetic capacity (Fig. 4, E and F). On DOY 193, the *Y11y11* canopy was more efficient throughout the entire vertical profile for most of the day, excepting short periods at the beginning and end of each photoperiod when oversaturation was low in both canopies due to low incident light levels. On DOY 230, the *Y11y11* canopy was more efficient throughout the entire

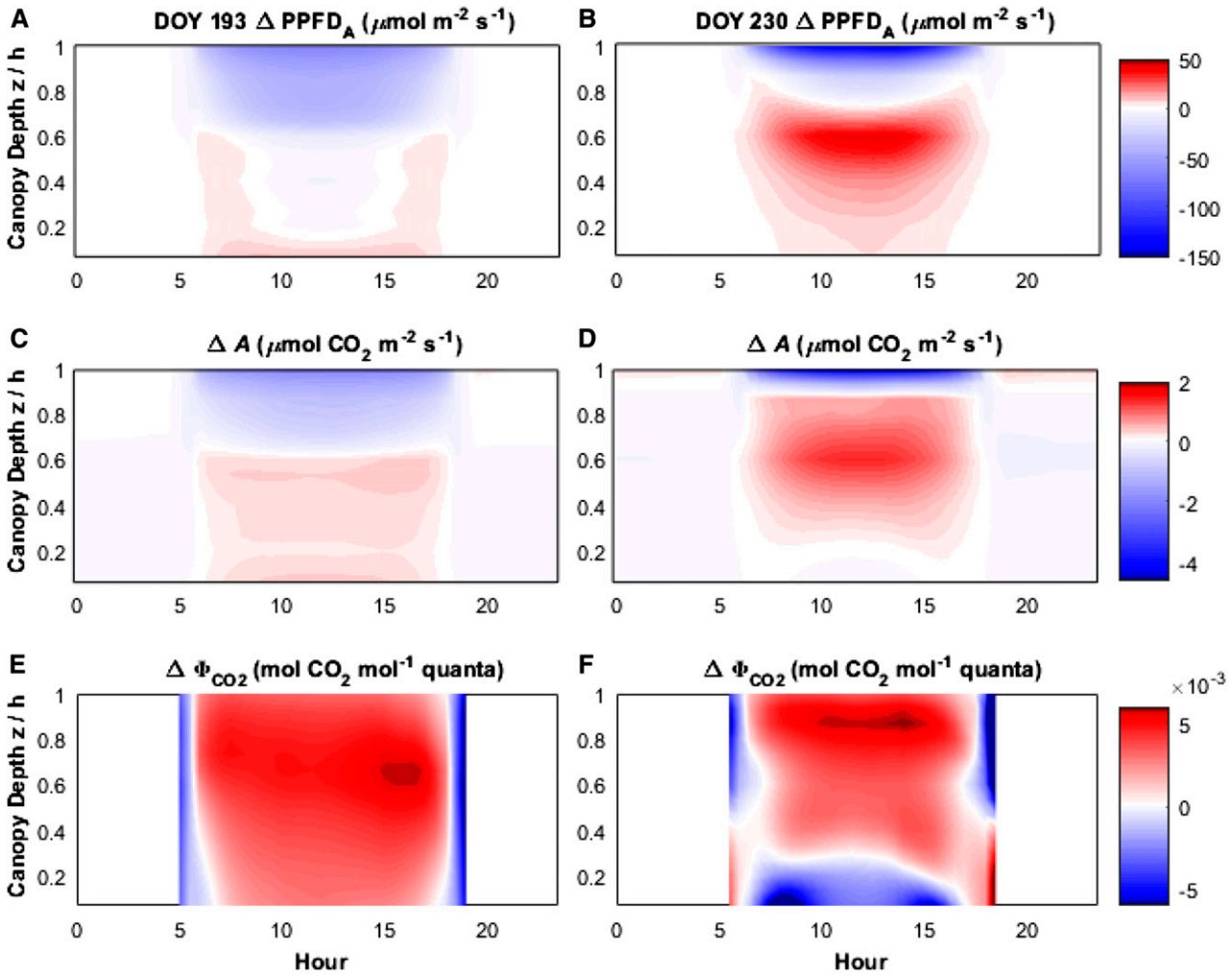

Figure 4. Vertically resolved, diurnal differences in absorbed PPFD ($\Delta PPFD_A$; A and B), net photosynthetic CO_2 assimilation (ΔA; C and D), and the quantum efficiency of CO_2 assimilation ($\Delta\Phi_{CO2}$; E and F) between a mutant with reduced chlorophyll content (*Y11y11*) and wild-type before canopy closure early in the growing season (DOY 193 LAI = 2.7: canopy A, C and E) and at peak LAI (DOY 230 LAI = 7.5: canopy B, D and F). Color map shows the difference between *Y11y11* and wild-type canopies (*Y11y11*, wild-type values) at each of the vertical canopy regions above ground normalized by the canopy height (z/h). Positive values (yellow/red) represent regions of the canopy where *Y11y11* has a larger value than wild type, and blue values are regions where the wild-type values are higher. The two selected days were both cloudless and received similar amounts of total downwelling radiation (Supplemental Fig. S5). Wild-type and *Y11y11* canopies were parameterized using genotype-specific chlorophyll contents and leaf area indices. Values are expressed on a ground area basis. WT, wild type.

vertical profile for most of the day, except for the bottom 20% of the canopy (Fig. 4f).

Daily Simulations of Wild Type and Y11y11 *in Response to LAI with Constant Meteorological Forcing to Assess the Impact of Biochemical Scaling with Chl and N Distribution*

We next repeated the simulations of Figure 4 to determine the impact of scaling biochemical capacity with Chl through a canopy with Chl (approximately 50% reduction) similar to *Y11y11*. Wild type was represented as high Chl = 400 μmol m^{-2} and *Y11y11* as low Chl = 200 μmol m^{-2} for each of the two assumed LAIs (less dense LAI = 2.7 m^2 m^{-2} and more dense LAI = 7.5 m^2 m^{-2}). The simulations using the averaged diurnal cycle of environmental forcing revealed a response similar to the season-long simulations when photosynthetic biochemical capacity was not scaled with Chl (Supplemental Fig. S8). In less dense canopies, high Chl canopies had higher $PPFD_A$ than low Chl canopies at every canopy layer, which in turn drove higher or equal A at every canopy layer (Supplemental Fig. S8, A and C). Interestingly, the higher $PPFD_A$ of high Chl canopies did not drive A as efficiently as low Chl canopies, as can be seen from the higher Φ_{CO2} of low Chl canopies at midday throughout much of the canopy profile (Supplemental Fig. S8E). In denser canopies, high Chl values produced higher $PPFD_A$ in the upper layers, but not in the lower, resulting in slightly higher A in the lower canopy of low Chl canopies, where effective shading by the upper canopy foliage was relatively reduced (Supplemental Fig. S8, B and D). As expected, the increased light distribution through the canopy resulted in a greater Φ_{CO2} of low Chl canopies through much of the canopy profile (Supplemental Fig. S8F). Interestingly, high Chl canopies had a slightly greater Φ_{CO2} in the very lowest regions of the canopy (Supplemental Fig. 8F).

However, when photosynthetic biochemical capacity was scaled according to Eqs. 3 and 4, A was reduced independently of differences in LAI (Supplemental Fig. S9, A to D). This resulted in large decreases in Φ_{CO2} in both LAI simulations during the majority of the day when light levels were highest (Supplemental Fig. S9, E and F). The regions of improved *Y11y11* net carbon exchange forecasted during night-time were a result of decreased modeled R_d, stemming from MLCan's use of V_{cmax} to estimate rates of R_d ($R_d = 0.015 * V_{cmax}$).

Seasonal Simulations of Wild Type and Y11y11

We next used this approach to examine the dynamics of $PPFD_A$ and A throughout the canopy across the entire 2013 growing season using observed forcing data from midday as measured in Champaign, IL. Figure 5 shows the differences between wild-type and *Y11y11* canopies over an almost 90-d period. The same general trends seen in the representative days presented in Figure 4 are seen throughout the growing season. Early and late in the season, there was little difference in $PPFD_A$ or A between wild type and *Y11y11*, except for slightly larger values for wild-type plants in the uppermost canopy layers (Fig. 5, a and c). As canopy density increased between DOYs 200 and 250, $PPFD_A$ and A were increased in the uppermost canopy layers of wild type relative to *Y11y11*, but the percentage of the vertical profile where *Y11y11* $PPFD_A$ and A was greater than wild type increased and peaked when LAI was the highest (approximately DOY 235; Supplemental Fig. S6e) during clear-sky conditions when radiation forcing was greatest. For the daily integrals of $PPFD_A$ and A over the duration of the growing season, wild-type canopies absorbed more PPFD (10%) and assimilated more carbon dioxide (4%) than *Y11y11* (Fig. 5, a, b, and d).

The seasonal Φ_{CO2} variations showed that *Y11y11* canopies were more light-use efficient than wild-type canopies at many canopy layers and on many days during the growing season (Fig. 6). With simulations parameterized with *Y11y11*-specific LAI values and using wild-type biochemical capacity, the vertical profile of Φ_{CO2} agreed with the diurnal profiles from single days, with increased Φ_{CO2} in *Y11y11* simulated at the upper canopy during periods when LAI was the highest (Fig. 6, a and b; Supplemental Figs. S6 and S8). The increased Φ_{CO2} for *Y11y11* in the upper canopy when biochemical parameters were held constant decreased in simulations performed using constant biochemical parameters and LAI and LAD values from wild-type canopies (Fig. 6c). With both assumptions of LAI, Φ_{CO2} appeared at first to increase in *Y11y11* as indicated by the more red regions of the vertical canopy across the season when photosynthetic biochemistry was scaled with Chl (Fig. 6, b and d). Although this simulation indicated a higher average Φ_{CO2} value in *Y11y11* with biochemical scaling, a closer examination revealed that the improvements in Φ_{CO2} occurred only when $PPFD_A$ and A_n were the lowest (Supplemental Fig. S10).

Using Synthetic Canopies To Explore a Range of Chl and Nitrogen Distributions

We next used the field data collected across the diverse soybean accessions to develop a second set of simulation experiments designed to quantify canopy performance as a function of leaf Chl. For these simulations of synthetic canopies, the observed LAI values from wild-type soybeans measured in the 2013 field season were used to allow us to focus on the impacts of varying Chl, photosynthetic biochemical capacity, and canopy nitrogen distribution. Chl was varied across a range representative of the natural variability seen in the experimental population (25 μmol m^{-2} to 500 μmol m^{-2}).

Impact of Assumptions of Leaf Optical Properties to Seasonal Radiative Regimes

Because PPFD reflected from the top of the canopy cannot be used for photosynthesis, the relationship

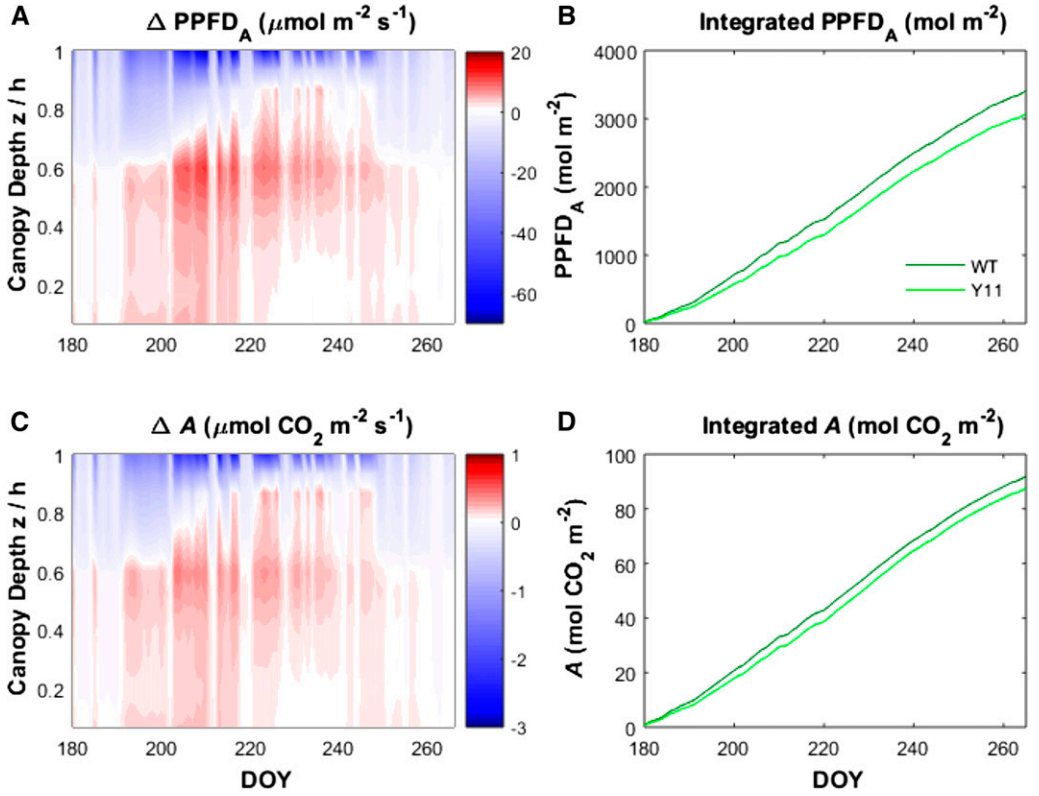

Figure 5. Vertically resolved differences in absorbed photosynthetically active radiation ($\Delta PPFD_A$, A) and net CO_2 assimilation (Δ, canopy A, C) between a simulated soybean canopy with reduced chlorophyll content (*Y11y11*) and a wild-type canopy, at midday time points for DOY spanning the growing season. Vertical profiles (height above ground normalized by canopy height, z/h) are presented for midday periods (1:00 PM) of each day throughout the growing season. Also shown are the seasonally integrated values for $PPFD_A$ (B) and A (D). Color map shows the difference between *Y11y11* and wild-type canopies (*Y11y11*, wild-type values) at each of the canopy regions, normalized by the canopy height (z/h). Positive values (more red) represent regions of the canopy where *Y11y11* has a larger value than wild type, and more blue values are regions where the wild-type values are higher. These simulations were driven by field-measured incident radiation, temperatures, and precipitation (see Supplemental Fig. S5). Wild-type and *Y11y11* canopies were parameterized using genotype-specific chlorophyll contents and leaf area indices (Slattery et al., 2017). WT, wild type.

between L_R and L_R with Chl (Fig. 2; Supplemental Fig. S2) translates to an increase in PPFD lost due to reflection as Chl decreases. To determine the total impact of increasing PPFD reflectance from the top of the canopy with decreasing Chl on canopy absorbance (Can_A), we simulated two distinct scenarios. In the first scenario (Fig. 7, a, c, and e), we scaled L_R with Chl according to Eq. 2. In the second scenario (Fig. 7, b, d, and f), we maintained L_R at a negligible value. L_R was always assumed to scale with Chl according to Eq. 1. Canopy optical properties were closely related to the leaf optical properties applied throughout the canopy, as well as total canopy LAI. Canopies with higher leaf Chl showed corresponding decreases in canopy transmittance (Can_T) and reflectance (Can_R; Figure 7, a, c, and e). Seasonal variations in LAI drove additional interactions, with the peak of the growing season resulting in significantly decreased Can_R and Can_T, as most PPFD was absorbed by the vegetation across all Chl levels for the canopy densities examined here. When L_R was modeled as negligible to assess the impact of increased albedo loss to Can_A in canopies with reduced Chl, there was very little Can_R compared to canopies with L_R scaled according to Eq. 2 (Fig. 7, a and b). The small amount of Can_R early and late season arose from the soil reflectance when the canopy was least dense. Decreased Can_R translated to increased Can_A in canopies with negligible L_R, especially when Chl was low (Fig. 7, e and d). Because these simulations characterize only the light environment of the canopy, they were not sensitive to different assumptions of photosynthetic capacity distribution or sensitivity to Chl.

Impact of Chl Reduction to Seasonal Canopy Photosynthesis

We next examined the impact of Chl variation on A_{can} and Φ_{CO2} with various assumptions of L_R Chl response and biochemical sensitivity (Fig. 8). Reductions in Chl decreased A_{can} under all simulated conditions except for when L_R was kept at a negligible value and biochemistry was not scaled with Chl, where A_{can} increased by a maximal approximately 2% when Chl was

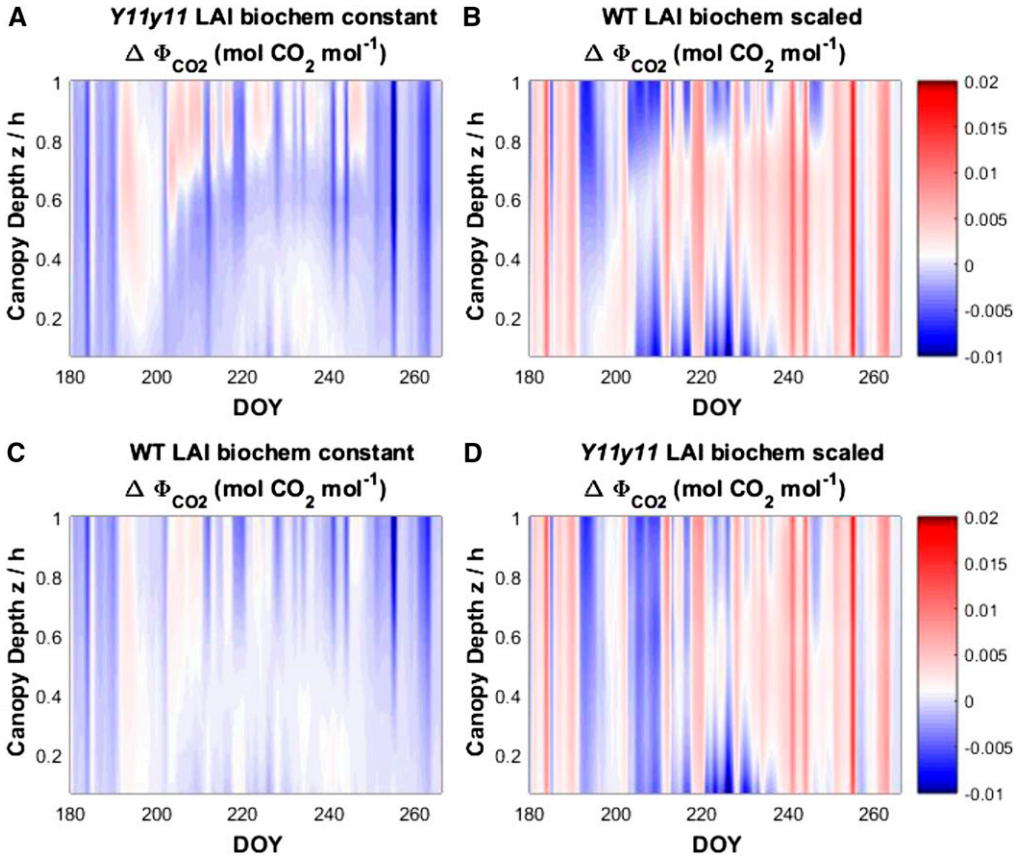

Figure 6. Season-long differences in the midday quantum efficiency of CO_2 assimilation ($\Delta\Phi_{CO2}$) between *Y11y11* soybean mutants (*Y11y11*) and wild type across the vertical profile of the canopies (height above ground normalized by canopy height, z/h) for the 2013 growing season. Color map shows the difference between *Y11y11* and wild-type canopies (*Y11y11*, wild-type values) at each of the canopy regions above ground normalized by the canopy height (z/h). Positive values (more red) represent regions of the canopy where *Y11y11* has a larger value than wild type, and more blue values are regions where the wild-type values are higher. Simulations were performed assuming the genotype-specific Chl content and *Y11y11* values for (A) LAI and constant photosynthetic biochemical capacity (V_{cmax} and J_{max}), (B) wild-type LAI and biochemical capacity scaled with Chl, (C) wild-type LAI and a constant photosynthetic biochemical capacity, and (d) *Y11y11* values for LAI and biochemical capacity scaled with Chl. Environmental forcing (precipitation, downwelling radiation, temperature, H_2O vapor pressure, and wind speed) for the simulations were taken from the 2013 growing-season. WT, wild type.

75 μmol m^{-2} (Fig. 8a; Supplemental Fig. S10). When photosynthetic capacity was held constant but L_R scaled with Chl, noticeable reductions occurred in A_{can} below 275 μmol m^{-2} (Fig. 8a). When leaf photosynthetic biochemical capacity was varied with Chl according to our empirical relationships, canopy performance was highly sensitive to Chl with a steep decrease in A_{can} along the simulated Chl gradient (Fig. 8a). Φ_{CO2} increased when photosynthetic biochemical capacity was held constant (Fig. 8b; Supplemental Fig. S10). In contrast, Φ_{CO2} generally decreased when leaf photosynthetic biochemical capacity decreased with Chl.

Combined Impact of Leaf Optics and N Distribution on Canopy Photosynthesis for a Representative Day

In MLCan, the vertical distribution of photosynthetic capacity is scaled with N assuming an exponential decay function containing k_n in the exponent (see "Materials and Methods"; De Pury and Farquhar, 1997). To determine if the greater Φ_{CO2} and PPFD penetration in the low Chl canopies could result in improved A_{can} by distributing biochemical capacity deeper into these regions, we next ran one-day simulations where Chl and nitrogen distribution were varied combinatorially. To modify nitrogen distribution, we used different values of the exponential decay term k_n (set as 0.5 as a default and in previous simulations) to determine the impact on canopy PPFD absorbance and performance among three different Chl contents (Supplemental Fig. S12). In these simulations the nitrogen distributions of different k_n assumptions were scaled so that total canopy nitrogen was not varied with k_n (see "Materials and Methods"). Higher k_n resulted in N more quickly decreasing with depth in the canopy (Supplemental Fig. S12). Additionally, decreased leaf

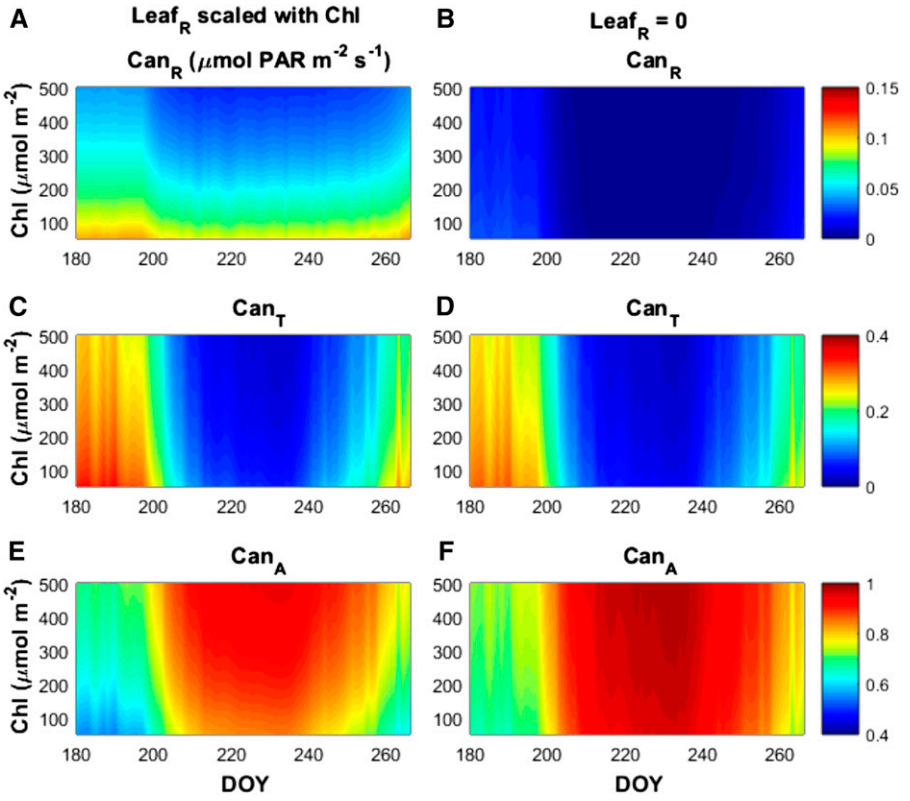

Figure 7. Total canopy reflectance (Can_R; A and B), transmittance (Can_T; C and D), and absorbance (Can_A; E and F) in simulated canopies composed of a range of leaf Chl content going from dark-green (500 μmol m^{-2}) to light-green (50 μmol m^{-2}) according to DOY within the growing season. Total values for each optical property were determined by summing the diurnal values for PPFD reflected, transmitted, or absorbed by the canopy divided by the summed total of diurnal incoming PPFD. Simulations were performed assuming leaf reflectance ($Leaf_R$)and transmittance ($Leaf_T$) covaried according to empirical relationships (A, canopy C, and E; Eqs. 1 and 2) derived from observations of diverse soybean lines (see Fig. 2) spanning a wide range of Chl as indicated by the decreasing Chl displayed on the *y* axis. Alternatively, canopies were simulated with $Leaf_R$ set to a negligible value at every Chl (B, D, and F) to show the impact of leaf reflective loss on total canopy optical properties.

Chl increased the proportion of PPFD absorbed in the lower canopy in the three Chl values shown (400, 200, and 50 μmol m^{-2}). There was good agreement with the N distribution and PPFD absorbance profiles at k_n values between 0.3 and 0.5 when Chl = 400 μmol m^{-2} and 200 μmol m^{-2}, whereas at the lowest Chl of 50 μmol m^{-2} the best agreement was observed at k_n values slightly less than 0.3. This suggests that the optimal nitrogen distribution, represented by k_n, should be somewhat sensitive to Chl.

To determine the combinatorial effect of nitrogen distribution and Chl to A_{can}, we performed daily simulations of A_{can} parameterized with different assumptions of A_{can} and k_n under average field data weather forcing and LAI = 7.5 m^2 m^{-2} (Fig. 9). These simulations confirmed that the k_n value that produces the highest A_{can} changes with Chl, as can be seen by the shifting regions of highest A_{can} as Chl decreased under both assumptions of L_R (Fig. 9). When L_R was scaled with Chl, the optimal k_n shifted from approximately 0.45 μmol m^{-2} at 500 μmol m^{-2} to approximately 0.35 at the lowest Chl values (Fig. 9a), in agreement with the values of k_n that produced nitrogen profiles in the closest agreement with $PPFD_A$ profiles (Supplemental Fig. S12). In all cases when L_R was scaled with Chl, A_{can} decreased with Chl, regardless of k_n (Fig. 9a). Consistent with the seasonal simulations (Fig. 8), A_{can} increased with reduced Chl when L_R was set to a negligible value (Fig. 9b). Interestingly, the increase in A_{can} was dependent on k_n, further demonstrating that L_R and N distribution conspire to impair the ability of Chl reductions to increase A_{can}.

DISCUSSION

Chl Reduction Alone Does Not Directly Improve Canopy Photosynthesis

Our findings predict that reductions in Chl are not expected to increase A_{can} by increasing light penetration into soybean canopies when the canopy is examined as a whole under realistic modeling assumptions (Fig. 8; Supplemental Fig. S10). However, a light-green canopy can have regions of greater $PPFD_A$ and A, resulting in increased Φ_{CO2} through much of the vertical canopy domain of light-green mutants (Figs. 4 to 6; Supplemental Fig. S8). For the simulations conducted here, the gains in Φ_{CO2} in the lower light-green canopy were not enough to offset the higher A of upper-canopy foliage in dark-green canopies. The increase in A found in the lower regions of the light-green canopy during the part of the growing season with peak LAI and greatest incident PPFD (Figs. 4 and 5) indicates that improvements to total light-green canopy performance could be realized if biochemical capacity were redistributed to better take advantage of redistributed PPFD (discussed further below). Our findings also indicate that Chl can be drastically reduced with little impact to A_{can}, suggesting an overinvestment in Chl and an

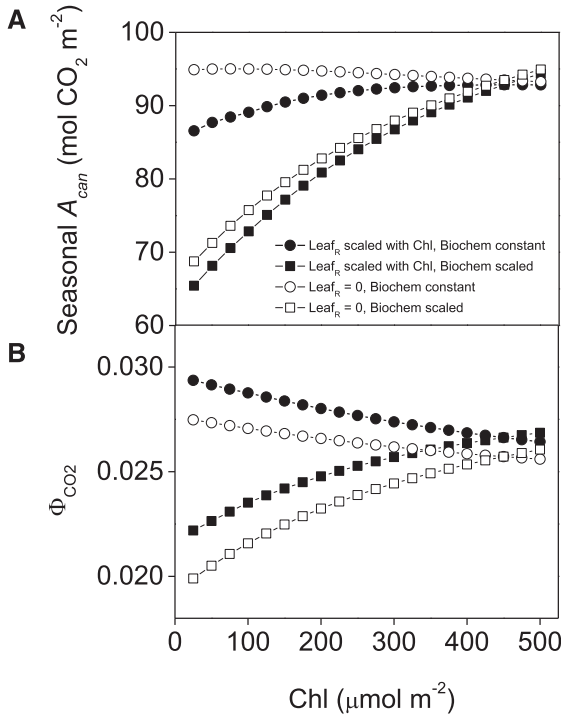

Figure 8. Impact of Chl content reduction on the seasonal simulated soybean photosynthesis (A_{can}; a) and the quantum efficiency of CO_2 fixation (Φ_{CO2}; b). Seasonal values are shown for the 2013 growing season (see Supplemental Fig. S5). Simulations were performed assuming leaf photosynthetic biochemical capacity remained constant despite chlorophyll content (Chl; circles) or that it scaled with Chl according to Eqs. 3 and 4 (squares). Leaf reflectance and transmittance were also assumed to both vary with Chl according to Eqs. 1 and 2 (solid symbols), while leaf reflectance remained constant despite changes in Chl (open symbols) to determine the impact of changes in reflective loss on canopy performance.

underutilization of photosynthetic biochemical capacity in much of the canopy space of modern soybean cultivars.

Nitrogen Distribution and the Future of Light-Green Canopies

The inability of light-green canopies to achieve increased A_{can}, despite increases in $PPFD_A$ and A in the lower canopy, partially results from the way photosynthetic biochemical capacity is distributed spatially through the canopy (Fig. 9; Supplemental Fig. S12). MLCan is coded to decrease photosynthetic biochemical capacity exponentially with canopy depth, according to the decay of nitrogen content found in a variety of crops and herbaceous plants including >16 cultivars of wheat, *Vicia faba*, *Oryza sativa*, *G. max*, *Sorghum bicolor*, *Amaranthus cruentus*, *Helianthus annuus*, *Hibiscus cannabinus*, *Cynara cardunculus*, and *Carex acutiformis* (Schieving et al., 1992; Anten et al., 1995; Anten, 1997; De Pury and Farquhar, 1997; Del Pozo and Dennett, 1999; Dreccer et al., 2000; Yin et al., 2003; Archontoulis et al., 2011; Moreau et al., 2012). Because of the lack of repartitioning the nitrogen profile in the simulations, the relative increase in availability of PPFD over the majority of the vertical canopy space in the low Chl canopy (Figs. 4 and 5) did not result in higher A_{can} partially because photosynthetic biochemical capacity was not repartitioned spatially to regions where the light-green canopy was most efficient, such as in the deepest canopy regions (Fig. 9). For example, on DOY 230, the lower 20% of the canopy absorbed more PPFD (Fig. 4b) but had a lower A (Fig. 4d), resulting in a lower Φ_{CO2} (Fig. 4f).

The optimal readjustment in nitrogen distribution would need to vary temporally (or with LAI) as illustrated from the differences in the example DOYs of Figure 4 to take best advantage of the redistributed PPFD in light-green canopies. Similarly, the simulations also revealed A_{can} did not increase with Chl reduction despite many combinations of Chl and k_n (Fig. 9a). It has also been proposed that a nitrogen reallocation within photosynthetic capacity has the potential to improve A within a single leaf in future climates based on modeling of optimal partitioning of V_{cmax} and J_{max} under future climate scenarios (Kromdijk and Long, 2016). The use of k_n to represent nitrogen distribution has not been conclusively linked to biological constraints, suggesting that other distributions are possible. Future work could explore direct optimizations of nitrogen distribution in the canopy with validation work in field-grown canopies to determine if more complex nitrogen distribution strategies could take better advantage of redistributed PPFD under current and future climates.

Although these simulations and field data do not support that Chl reductions would result in higher A through more optimal light distribution when implemented alone or even with redistributions of nitrogen across the canopy profile, they do indicate that a canopy can accommodate drastic reductions of Chl (as low as 16% of wild type), with only minimal impacts on A_{can}. If a plant could have similar A with less investment in nitrogen associated with Chl (both directly in Chl and in Chl-associated protein complexes), this would free-up nitrogen to be remobilized from antennae complexes to more limiting processes within the leaf. Indeed, leaf nitrogen seems to be conserved despite the reduced Chl of *Y11y11* (Supplemental Fig. S7), meaning that nitrogen assimilation and uptake in soybean is not sensitive to the demand based on chlorophyll biosynthesis. Although it is not clear where nitrogen is diverted to in reduced Chl mutants, this nitrogen could have substantial benefits if reinvested into photosynthesis, especially because many of the enzymes involved in carbon metabolism appear to have limiting suboptimal activities (Zhu et al., 2007). For example, a reduction of Chl from 500 to 100 μmol m^{-2} would result in a savings of 400 μmol m^{-2}, which translates to a nitrogen savings of 0.17 g nitrogen m^{-2}, assuming all the reduced Chl was bound to the light harvesting complex for photosystem II, the lowest nitrogen containing chlorophyll binding protein (0.42 g N mmol

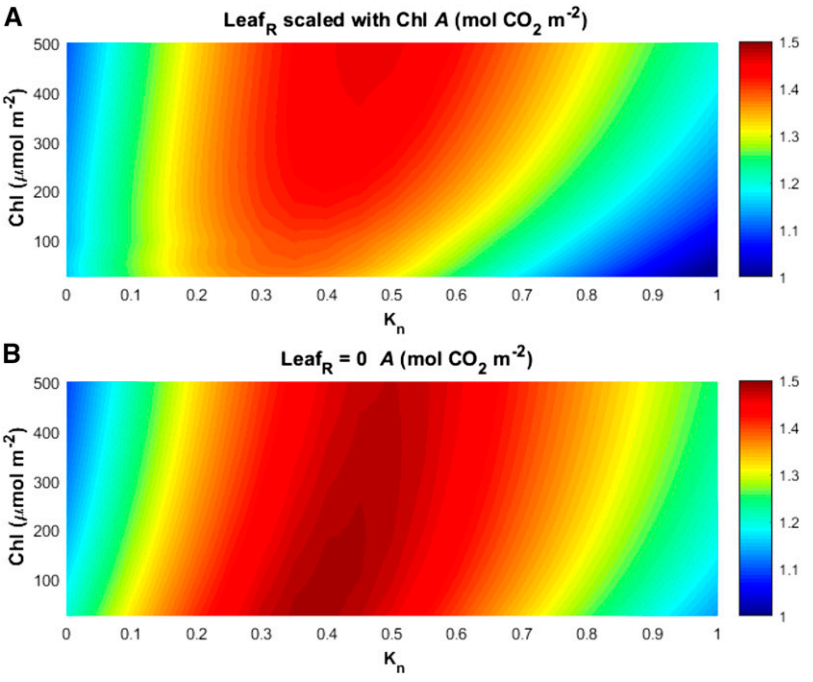

Figure 9. The response of total daily canopy carbon assimilation (A_{can}) to different assumptions of Chl and canopy nitrogen distribution profiles. Canopy nitrogen profiles were adjusted through varying k_n, a term describing the exponential decay of nitrogen through a canopy profile (see Supplemental Fig. S7 and "Materials and Methods" for more detail). Environmental forcing (radiation, temperature, relative humidity, etc.) was taken as the average daily conditions for the 2013 growing season. Shown are the relationships among Chl, N distribution, and canopy A, assuming leaf reflectance ($Leaf_R$) and transmittance ($Leaf_T$) covaried according to empirical relationships (A) and assuming Leaf$_R$ was negligible (B).

Chl^{-1}). This would represent an 8% to 12% savings in total leaf nitrogen, assuming the wild-type leaf N contents we measured during the field season (Supplemental Fig. S7). Such nitrogen savings could have a sizable positive impact on yield, because even nitrogen-fixing *G. max* is often nitrogen-limited (Salvagiotti et al., 2008). It is interesting that in *Y11y11*, the nitrogen saved from reduced Chl investment is still maintained by the leaf as evidenced by the identical nitrogen and protein contents of both genotypes for all but one sampling day (Supplemental Fig. S7), raising the question of where nitrogen is mobilized in reduced Chl plants if not to photosynthesis.

The positive impact of redirecting nitrogen from Chl to limiting enzymes in photosynthesis was recently demonstrated in a simulated rice canopy using a ray-tracing algorithm coupled to a complete biochemical representation of C_3 photosynthesis (Song et al., 2017). In this model, there was only a modest benefit of reducing Chl content alone (Approximately 3% increase in A_{can}), but when the saved nitrogen was reinvested in limiting enzymatic steps of C_3 photosynthesis, both A_{can} and nitrogen use efficiency could be increased by 30%. The next logical step for canopy optimization through canopy Chl reduction is therefore to understand where nitrogen is partitioned in plants with reduced Chl and how this repartitioning can be more optimally engineered. In addition to the coupled ray-tracing and C3 metabolic model of Song et al. (2017), there are additional frameworks for repartitioning nitrogen based on five competing photosynthetic sinks using a colimiting model parameterized by empirically derived relationships (Hikosaka and Terashima, 1995). This particular model, however, is not compatible with MLCan because MLCan uses the mechanistic biochemical relationships of photosynthesis to simulate canopy response to radiation and atmospheric conditions. The relationship between Chl and V_{cmax} and J_{max} indicate that nitrogen reallocation from antenna complexes to photosynthetic biochemical capacity does not happen generally as a result of mutations that reduce Chl (discussed further below), but it is possible that more targeted engineering strategies could help achieve this goal.

Tradeoffs between Leaf Reflectance and Transmittance Limit the Benefits of Light-Green Canopies

The inability of Chl reductions to increase canopy light penetration enough to increase A also partially results from the observed relationship between L_R and L_R (Fig. 2; Supplemental Fig. S2). Both L_R and L_R increase with decreasing Chl because both originate from the scattering of light within the complex inner anatomy of the leaf due to the differences in the refractive indices between air (1.00) and cell material (approximately 1.48; Woolley, 1971). Thus, L_R and L_R only differ in the direction of the light scattering and result from the many air-to-cell interfaces within a leaf (Woolley, 1971; Terashima and Saeki, 1983), a relationship confirmed in our observations (Fig. 2; Supplemental Fig. S3). The largest amount of reflected PPFD occurs from the upper canopy layer, where incident radiation is greatest. Reflected PPFD from the upper canopy is lost from the canopy and not available to drive A, resulting in decreased Can_A (Fig. 7e). The decrease in Can_A is not fully compensated for by increases in Φ_{CO2} when L_R and L_R are set equal to the relationships in Eqs. 1 and 2 (Fig. 8b), resulting in decreased A in lower Chl canopies (Fig. 8a).

Only when L_R is reduced to a negligible value do simulated reduced Chl canopies have greater A_{can} (Figs. 8a and 9b), demonstrating that the increased reflective loss of PPFD from the leaf surface accompanying Chl reduction partially explains their reduced A_{can}.

The ability of light-green canopies to increase A when L_R is reduced to a negligible value may help explain why Chl reductions in algal cultures have resulted in increased photosynthesis and growth culture (Melis, 1999; Polle et al., 2003; Mitra and Melis, 2008; Kirst et al., 2012). In *Chlorella* cultures, light absorption is well represented by the Beer-Lambert law at a variety of cellular densities, without the necessity for consideration of reflectance (Lee, 1999). The difference in reflective properties between a leaf and an algal culture could be the result of both the decreased differences in refractive indices between the algal cell (1.047 to 1.092; Spinrad and Brown, 1986) and the aqueous culture medium (1.33) compared to leaves and the less cell-dense culture conditions, which minimize cell-to-medium light scattering. For example, in the experiments of Kirst et al. (2012), that reported improved growth of *Chlamydomonas reinhardtii* with reduced antenna complexes, cells were cultured at densities 1–3 $\times$ 10^6 cells mL^{-1}. Leaf cell density is not reported directly, but can be approximated based on available data. Based on anatomical data, a single soybean leaf has approximately 2.5 $\times$ 10^6 cells cm^{-2} in the palisade layers alone (Dornhoff and Shibles, 1976). Spongy mesophyll cells are smaller than palisade cells but are not packed as tightly. Assuming their cellular density per leaf surface area is similar to palisade cells, this means that a single leaf layer has a similar order of magnitude of light-scattering cells as a cm^3 of algal culture. Additionally, leaves are arranged in a variety of angles relative to each other, which would further serve to increase canopy light scattering. Due to these fundamental differences between the culture properties of algae and plants, it is impossible to completely separate L_R from L_T, but even reducing the relationship between the two would increase A_{can} in reduced-Chl canopies relative to canopies with L_R according to Eq. 2.

Theoretically, L_T and L_R could be separated from each other if internal leaf architecture were simplified to limit the amount of cell-to-air interfaces. This could be accomplished by decreasing the cell number or complexity of the intercellular airspace, such as is seen in the *reticulata* mutants in Arabidopsis (González-Bayón et al., 2006). However, this may negatively impact the efficiency of internal CO_2 diffusion and subsequent leaf photosynthesis (Syvertsen et al., 1995; Evans and von Caemmerer, 1996; Flexas et al., 2007).

The Relationship between Chl and Photosynthetic Capacity Gives Insight to Past Work with Light-Green Canopies

We identified an important correlation between Chl and photosynthetic biochemical capacity (J_{max} and V_{cmax}) found in naturally and chemically derived soybean accessions that drastically alters the impact of Chl reduction on canopy performance (Figs. 3 and 8; Supplemental Figs. S8, S9, and S11). The correlation between Chl and V_{cmax} had a higher y-intercept and lower slope than a relationship based on predicted N content and secondary relationships, suggesting that the model of Houborg et al. (2013) may not apply well at least to soybean. The driver linking Chl to J_{max} and V_{cmax} is currently not known, but there were cultivars that had reduced Chl without a corresponding decrease in photosynthetic biochemical capacity in the 45 lines we surveyed with gas exchange (Fig. 3). A similar inconsistent relationship between Chl and biochemical capacity was seen across soybean cultivars with years of release dates between 1923 and 2007 (Koester et al., 2014). The presence of accessions with high biochemical capacity and low Chl indicates there is not an underlying genetic linkage or immutable mechanism that links the two, and that the correlation can be avoided. The relationship between Chl and photosynthetic biochemical capacity found in naturally and chemically derived soybean accessions would hamper efforts to breed for reduced chlorophyll production lines through traditional methods, and highlights the need for targeted genetic markers or genetic engineering.

Although our findings show that, in general, Chl is correlated with biochemical performance measured as V_{cmax} and J_{max} across a broad panel of soybean mutant accessions, the case may be different in other species and dependent on the genetic and biochemical source of the mutation. A rice mutant with greatly reduced Chl was reported to have large increases in both V_{cmax} and J_{max} (Gu et al., 2017a, 2017b). Canopies of this mutant had significant increases in A_{can}. The differences between our results in soybean and this single mutant in rice could indicate species-specific differences in how nitrogen is repartitioned when chlorophyll production is impaired, or simply that the mutant they used for their study represents an exception to the general trend. Our simulations predict that the increased A_{can} of this light-green rice cultivar was likely due more to the increases in V_{cmax} and J_{max} and not from PPFD redistribution. Indeed, the rice mutant has higher A_{leaf} at saturating irradiances, indicating that the leaf capacity for photosynthesis was greater than wild type.

Furthermore, a *Nicotiana tabacum* mutant with substantially reduced Chl also reported an increase in biomass yield when grown in dense stands (Kirst et al., 2017). The discrepancy between this modeling work in soybean and this recent report in *N. tabacum* could be attributed to a variety of reasons. Our simulations were parameterized specifically for field-grown soybean, and differences in leaf thickness, arrangement, and weather conditions (the *N. tabacum* was grown in a greenhouse) could impact the results. Additionally, the *N. tabacum* mutants were harvested several days after the wild type to make up for developmental differences, which could confound the interpretation of the measured increases in biomass. Taken at face value, our

simulations indicate that the increase in growth found in *N. tabacum* likely resulted from factors other than just canopy PPFD redistribution, such as developmental differences or increases in V_{cmax} and/or J_{max} as was found in the rice cultivar.

Pleiotropic Effects of Chl Reduction

Because past work with *Y11y11* indicates that chlorophyll reduction can be accompanied with an increase in stomatal conductance (Campbell et al., 2015; Slattery et al., 2017), what other pleiotropic effects might be expected from reduced chlorophyll mutants? Chlorophyll precursors are derived from the isoprenoid pathway, which also is involved in the biosynthesis of a myriad of plant secondary metabolites including carotenoids, gibberellins, and tocopherols (Lange and Ghassemian, 2003). Because chlorophyll reduction could be caused by any perturbation downstream of final chlorophyll biosynthesis, it is possible that molecules that share chlorophyll's biosynthetic pathway could be impacted in reduced chlorophyll plants. For example, there was a strong correlation between Chl and total carotenoid content (Supplemental Fig. S2A) that resulted in more carotenoids per chlorophyll at low Chl (Supplemental Fig. S2 similar to the relationship found in *Coffea canephora* Pierre leaves (Netto et al., 2005). Carotenoids play a role in regulating nonphotochemical quenching and harvesting light energy in spectral regions that chlorophyll does not absorb strongly (Ort, 2001; Telfer et al., 2008), indicating that these processes might be impacted in low Chl mutants. Interestingly, lower carotenoid content also correlates with ABA levels in plants with transgenically impaired carotenoid synthesis (Lindgren et al., 2003). Whereas ABA triggers stomatal closure (Farquhar and Sharkey, 1982), the relationship between carotenoid content and stomatal closure was not apparent in the 45 accessions that were examined via gas exchange (Supplemental Fig. S5a). Chl reduction may also reduce the quantity of reactive oxygen species generated from overexcited reaction centers (Vass and Cser, 2009) by reducing total light energy absorption, perhaps resulting in surplus antioxidant capacity and improved stress response (Foyer and Shigeoka, 2011).

CONCLUSIONS

Our findings indicate that whereas reductions in Chl alone are not expected to increase A in soybean, they can result in increased Φ_{CO2} and carbon fixation in individual domains of the canopy. The inability of Chl reduction to increase canopy photosynthesis results primarily from the fundamental linkage between L_R and L_T, with the vertical distribution of nitrogen being a secondary factor. Nevertheless, our simulations show that canopies can assimilate similar amounts of carbon dioxide with significant reductions in Chl. Future efforts should focus on repartitioning nitrogen from excess chlorophyll into more beneficial investments, such as V_{cmax} and J_{max}.

MATERIALS AND METHODS

Field Measurements for MLCan Parameterization

Soybean germplasm (67 lines) with previously described "light-green" phenotypes were planted in 1.5-m rows using standard agronomic practice (specific lines listed in Supplemental File S1). Seed was obtained from the United States Department of Agriculture Soybean germplasm collection and from the Fast Neutron Soybean Mutagenesis Project (http://parrottlab.uga.edu/parrottlab/Mutagenesis/index.php) and when available, included the parental lines of the light-green cultivar. Due to seed limitations, a single row of each variety was planted in a single randomized block, with edges bordered by wild-type soybean (*Glycine max* Merr., cultivar "Clark") rows. Leaves for analysis were harvested at two points in the growing season by predawn cutting from the plant followed by recutting the petioles under water. Plants were then transferred in a darkened container to the lab for Chl, total carotenoid, and optical property determination. L_R, L_T, L_A, and SPAD (Soil Plant Analysis Development; Chlorophyll Meter SPAD-502 Plus; Konica Minolta) were determined on three to five replicates of each line and Chl was determined on the same area using ethanol extraction (Ritchie, 2006). The relationship used to convert SPAD readings to Chl was calculated using an exponential function (Supplemental Fig. S13). Leaf optical properties were determined using an integrating sphere and spectroradiometer using a tungsten-halide source (Jaz Spectroclip; Ocean Optics) with a source in the visible range although it should be noted that the source has reduced output between approximately 400 nm and 500 nm, meaning that the measurements of blue light are less reliable than that for the other colors. The integrating sphere/spectroradiometer was first calibrated with a Spactralon 99% reflectance standard (Labsphere) and the black standard included with the instrument. Dark-adapted and steady-state fluorescence were measured using a fluorescence camera on leaf disks placed on agar plates.

The relationships between leaf optics and Chl that were used to define leaf optical properties in MLCan as a function of Chl were:

$$Leaf_T = 0.228e^{-0.00288(Chl)} \quad (1)$$

($R^2 = 0.50$) and

$$Leaf_R = 0.208e^{-0.00217(Chl)} \quad (2)$$

($R^2 = 0.52$). The R^2 values of the relationships between Chl and leaf optics (Eqs. 1 and 2) indicate that there are factors impacting leaf optics other than Chl. This is to be expected given the diverse genetic nature of the soybean accessions measured and the complex interaction of leaf anatomy with incident PPFD (Osborne and Raven, 1986) as well as measurement noise. Indeed, past work measuring the relationship of Chl with L_A observe a similar degree of variance (Osborne and Raven, 1986; Evans and Poorter, 2001). For our simulations, we assumed that these other factors would be constant in a leaf where only the Chl was reduced and used the above equations to simulate the impact of Chl on leaf optics.

The response of A_{leaf} to carbon dioxide concentration (A-C_i) was measured in the light-green and parental cultivars to determine the relationship between Chl and photosynthetic biochemical capacity (V_{cmax} and J_{max}). A subset of 45 cultivars was selected with a wide variation in Chl for measurements and harvested by predawn petiolar cutting and kept under partial (between 20 PPFD and 200 PPFD) illumination before measurements. A full A-C_i curve was measured for each cultivar using a model no. 6400XT (LI-COR Biosciences) and SPAD measured as a proxy for Chl. SPAD estimates of Chl based on the above calibration (Supplemental Fig. S13) were used because leaf samples were not harvested for direct determination. Measurements were made using a 2 cm^2 measuring area, a flow rate of 300 $\mu mol\ s^{-1}$, and CO_2 reference concentration sequence of 400, 300, 200, 100, 50, 400, 600, 800, 1000, 1300, and 400 PPM CO_2. The instrument's block temperature was maintained at 3° below ambient temperature, resulting in leaf temperatures between 25° and 30° depending on the time of day the measurement was made. Measurements were randomized and limited to the hours between 9:00 and 14:00 to avoid end-of-day photosynthetic depression. V_{cmax} and J_{max} were determined by fitting A-C_i curves and normalized

to 25°C using the temperature response of each determined previously for *Nicotiana tabacum* (Bernacchi et al., 2001, 2002, 2003; Sharkey et al., 2007). The relationship between V_{cmax} and Chl produced from this dataset was

$$V_{cmax} = 0.17(Chl) + 67.2 \quad (3)$$

with an R^2 of 0.27, and the relationship between J_{max} and Chl was

$$J_{max} = 0.33(Chl) + 113.4 \quad (4)$$

with an R^2 of 0.54.

Leaf nitrogen content was measured in field-harvested samples of wild type and *Y11y11* from the 2013 season on five different growing days. Samples were oven-dried for 3 d and ground using a ball mill (BT&C; Geno/Grinder) and analyzed using an elemental analyzer (4010CHNSO Analyzer; Costech Analytical Technologies). Acetanilide (National Institute of Science and Technology) was used as a standard.

Leaf soluble protein content was determined by the Bradford method (Bradford, 1976). Samples (1-cm diameter leaf disk) were collected in three plots during the 2013 season over four growing days. Tissues were rapidly frozen in liquid N, stored at −80°C, and ground by using a glass homogenizer while frozen. After extraction buffer was added, extracts were centrifuged at 18,000*g* at 4°C for 5 min. Supernatants were collected and mixed with a protein assay dye (Bio-Rad). Absorbance of samples along with bovine serum albumin as a standard was measured at 595 nm by microplate reader (BioTek).

Implementing the Impact of Chl into MLCan

MLCan treats PAR as a single broadband radiation stream by dividing total downwelling radiation between long and shortwave, then further partitioning shortwave radiation between PAR and near infra-red (Campbell and Norman, 1998; Drewry et al., 2010a). We measured leaf optical properties (L_R, L_T, and L_A) at approximately 34 nm resolution across the PAR portion of the spectrum (400 nm to 700 nm), requiring us to aggregate leaf spectral properties to broadband PPFD values. To do this, L_R, L_T, and L_A were averaged into 25-nm increments between 400 nm and 700 nm. Twenty-five nanometers were selected as an interval because it gave reasonable resolution across both the chlorophyll absorption spectra and the solar spectra for weighted averaging. L_R, L_T, and L_A for each 25-nm value were then multiplied by the percentage of solar radiation incident relative to the total PAR solar radiation using a reference solar spectrum, to produce weighted values (L_R, L_T, and L_A; ASTM, 2012). The weighted L_R, L_T, and L_A values from each 25-nm increment were then summed to produce a weighted average across the PAR spectrum, which was then fit to produce empirical allometric relationships between optical properties and Chl (Eqs. 1 and 2).

Equations 1 and 2 were used to vary leaf-level optics based on the value of Chl used in MLCan. To accomplish this, MLCan was modified so that L_R, L_T, and L_A were varied for each 30-min time step, instead of being assigned as constant default values. In the first series of simulations representing wild-type and *Y11y11* canopies, time-step-specific Chl was interpolated from values measured for each genotype throughout the growing season (Slattery et al., 2017). L_R and L_T were calculated for each time step using Eqs. 1 and 2, and L_A determined according to $1 - L_R - L_T$.

Because the relationships of L_R and L_T were determined as a function of Chl, MLCan was modified to incorporate the individual relationships of both. MLCan, like many canopy models, assumes that L_R is equal to L_T, which simplifies the derivation of the extinction and scattering of radiation throughout the canopy. Leaf-level optics were scaled to the canopy-layer level by using a PPFD extinction (K_h) and reflectance (ρ_h) coefficient that considered L_R was not equal to L_T, allowing us to individually vary both parameters. Specifically, the original MLCan formulation of

$$K_h = (1 - \sigma)^{0.5} \quad (5)$$

where σ represents a scattering coefficient equal to $L_R + L_T$ and assuming $L_R = L_T$, was replaced with

$$K_h = \left(\left[1 - Leaf_T\right]^2 - Leaf_R{}^2\right)^{0.5} \quad (6)$$

and

$$\rho_h = \frac{1 - (1 - \sigma)^{0.5}}{1 + (1 - \sigma)^{0.5}} \quad (7)$$

was replaced with

$$\rho_h = \frac{\left(1 - Leaf_T - K_h\right)^{0.5}}{Leaf_R} \quad (8)$$

Details on the derivation of the equations and their use in MLCan can be found in Eqs. 2.20 to Eq. 2.23 in Goudriaan (1977) and Supplemental Eq. 23 in Drewry et al. (2010a). For each time-step, radiation was distributed through the canopy iteratively until all incoming radiation was either absorbed by a canopy layer or the soil, or reflected into the atmosphere to account for the intercanopy scattering and absorbance of incoming light. Soil reflectance was assumed to be 0.2.

In simulations including a scaling of V_{cmax} and J_{max} with Chl, leaf biochemistry was modified as a function of Chl for each time step using the empirical measurements according to Eqs. 3 and 4. This did not impact the simulations where Chl was constant throughout the growing season, but did have an impact when the wild-type and *Y11y11* canopies were simulated using field-measured seasonal Chl values. In all simulations Chl was considered constant through the canopy with no developmental-dependent effects. The vertical distribution of Chl was not accounted for, meaning that all leaves had the same assumed Chl for a given time step. For simulations determining the impact of uncoupling L_R from L_T, L_R in Eq. 2 was maintained at a constant value for Chl of 450 μmol m^{-2}, whereas L_T varied according to Eq. 1 and L_A determined as $1 - L_R - L_T$.

All meteorological, physiological, and ecological data are available by contacting B.J.W. For access to MLCan code, contact D.T.D.

Simulations Comparing a Wild-Type and *Y11y11* Canopy

Field measurements from the 2013 growing season were used to parameterize the canopy simulations of wild-type and *Y11y11* soybean canopies. Seasonal leaf area density, LAI, and Chl were taken from field measurements as reported previously (Slattery et al., 2017). Photosynthetic biochemical parameters (V_{cmax} and J_{max}) were assumed as outlined in the various modeled scenarios. Precipitation data were taken from the nearby Willard Airport weather station with radiation, windspeed, and temperature from other nearby sources as reported previously (Bagley et al., 2015).

It was a particularly wet spring with little additional precipitation during the growing season and the modeled soil moisture drove an end-of-season modeled stomatal closure. Modeled soil moisture did not agree well with field measurements, so the soil-model was constrained to never drop below measured values in the *Y11y11* or the full Chl simulations. Soil moisture was measured on a biweekly basis in a nearby plot of soybean (*cv* Pana, PI 597387) using a capacitance probe (Diviner-2000, Sentek Sensor Technologies) inserted into access tubes. Measurements were made in three access tubes at 10 cm increments between depths of 5 and 105 cm and averaged together to constrain the model. The raw data were converted to gravimetric data using a calibration determined in prepared soils (Paltineanu and Starr, 1997).

Simulating the Impact of a Range of Chl and Nitrogen Distribution on Canopy Performance

To determine canopy performance under a wider range of Chl, the 2013 season was simulated using Chl ranging from 25 μmol m^{-2} to 500 μmol m^{-2}. This simulation was done both assuming and not assuming that V_{cmax} and J_{max} scale according to Chl and assuming that L_R was maintained at a value calculated when Chl = 450 μmol m^{-2} (Eq. 2).

The impact of changes to the distribution profile of nitrogen to canopy performance was investigated in MLCan by altering the coefficient for the exponential function that represents the distribution of nitrogen through the canopy. Specifically, MLCan represents the canopy nitrogen profile, which scales V_{cmax} and J_{max} through the canopy as a function of nitrogen, according to the relationship

$$V_{cmax}(\xi) = V_{cmax}{}^{top}\exp[-k_n{*}\xi] \quad (9)$$

where ξ, V_{cmax}, and $V_{cmax}{}^{top}$ is equal to the cumulative LAI, V_{cmax} at the layer being modeled and the V_{cmax} at the top of the canopy, respectively (De Pury and Farquhar, 1997). To not include the effects of having more or less total nitrogen

in a canopy as a result of changing k_n, MLCan was amended to use the relationship above with the default value of k_n = 0.5 to first produce a baseline canopy nitrogen content. This baseline total nitrogen content was then scaled according to the relationship above to produce canopies with the same total amount of nitrogen but different profiles.

Supplemental Data

The following supplemental materials are available.

Supplemental Figure S1. Ratio of leaf transmittance (L_T) to reflectance (L_R) as a function of chlorophyll content.

Supplemental Figure S2. Relationship between Chl content and total carotenoid content (a) and the ratio of carotenoid to Chl across the 67 reduced-Chl accessions as measured on two separate field days.

Supplemental Figure S3. Relationship between Chl content and leaf reflectance ($Leaf_R$, a) and transmittance ($Leaf_T$, b) determined from 67 soybean accessions with varying amounts of Chl.

Supplemental Figure S4. Relationship between maximum variable fluorescence and electron transport rate.

Supplemental Figure S5. Impact of variation in Chl content on stomatal conductance (g_s) and rates of day respiration (R_d) in 45 plants from various cultivars of soybean as measured by fitting photosynthetic CO_2 response curves.

Supplemental Figure S6. Season-long incident photosynthetic photon flux density (PPFD; a), air temperature (b), precipitation (c), and H_2O vapor pressure (d) as measured in Slattery et al. (2017) and used to parameterize our season-long simulations.

Supplemental Figure S7. Seasonal values for measured leaf N, measured Chl content, calculated nitrogen associated with Chl (N in Chl; g m^{-2}), and a lower bounds calculation of the percent leaf nitrogen associated with Chl (N in Chl; %) for DOY.

Supplemental Figure S8. Diurnal differences in absorbed PPFD ($\Delta PPFD_A$; a and b), net photosynthetic CO_2 assimilation (ΔA; c and d), and the quantum efficiency of CO_2 assimilation ($\Delta\Phi_{CO2}$; e and f) between canopies with chlorophyll content (Chl) = 400 and Chl = 200 representing wild-type and reduced Chl mutants.

Supplemental Figure S9. Diurnal differences in absorbed PPFD radiation ($\Delta PPFD_A$; a and b), net photosynthetic CO_2 assimilation (ΔA; c and d), and the quantum efficiency of CO_2 assimilation ($\Delta\Phi_{CO2}$; e and f) between canopies with chlorophyll content (Chl) = 400 and Chl = 200 representing wild-type and reduced Chl mutants.

Supplemental Figure S10. Season-long relationships between the daily midday differences in the quantum efficiency of CO_2 assimilation ($\Delta\Phi_{CO2}$) among *Y11y11* soybean mutants and wild-type and net carbon assimilation (A_n; a) and absorbed photosynthetic photon flux density ($PPFD_A$; b).

Supplemental Figure S11. Impact of Chl content reduction on carbon fixation in simulated soybean canopies.

Supplemental Figure S12. Impact of changes to the coefficient of nitrogen distribution (k_n) on the vertical distribution of nitrogen through the canopy profile compared to the PPFD absorbed normalized to the uppermost canopy layer of nitrogen partitioning or absorption.

Supplemental Figure S13. Relationship between SPAD and Chl content as measured in various soybean cultivars with differing Chl.

Supplemental Data. Cultivars and gas exchange measurements.

ACKNOWLEDGMENTS

Jessica Ayers, Beau Barber, Kaitlin Togliatti, and Elliot Brazil are acknowledged for assistance sampling and measuring the population of reduced Chl cultivars. Christopher Montes is acknowledged for providing the soil moisture data from an adjoining plot at the Soybean Free Air Concentration Enrichment site. Randall Nelson (Retired) of the USDA is acknowledged for providing the light-green soybean accessions. Anastasiia Bovdilova is acknowledged for providing the Russian translation of early references to light-green in the literature.

Received September 26, 2017; accepted October 18, 2017; published October 23, 2017.

LITERATURE CITED

Ainsworth EA, Rogers A, Leakey ADB, Heady LE, Gibon Y, Stitt M, Schurr U (2007) Does elevated atmospheric [CO_2] alter diurnal C uptake and the balance of C and N metabolites in growing and fully expanded soybean leaves? J Exp Bot **58:** 579–591

Anten NPR (1997) Modelling canopy photosynthesis using parameters determined from simple non-destructive measurements. Ecol Res **12:** 77

Anten NPR, Schieving F, Werger MJA (1995) Patterns of light and nitrogen distribution in relation to whole canopy carbon gain in C_3 and C_4 mono- and dicotyledonous species. Oecologia **101:** 504–513

Archontoulis SV, Vos J, Yin X, Bastiaans L, Danalatos NG, Struik PC (2011) Temporal dynamics of light and nitrogen vertical distributions in canopies of sunflower, kenaf and cynara. Field Crops Res **122:** 186–198

ASTM (2012) G173 - 03(2012): Standard Tables for Reference Solar Spectral Irradiances: Direct Normal and Hemispherical on 37° Tilted Surface. ASTM International, West Conshohocken, PA

Bagley J, Rosenthal DM, Ruiz-Vera UM, Siebers MH, Kumar P, Ort DR, Bernacchi C (2015) The influence of photosynthetic acclimation to rising CO_2 and warmer temperatures on leaf and canopy photosynthesis models. Global Biogeochem Cycles **29:** 194–206

Baker NR (2008) Chlorophyll fluorescence: a probe of photosynthesis *in vivo*. Annu Rev Plant Biol **59:** 89–113

Baldocchi DD, Wilson KB, Gu L (2002) How the environment, canopy structure and canopy physiological functioning influence carbon, water and energy fluxes of a temperate broad-leaved deciduous forest—an assessment with the biophysical model CANOAK. Tree Physiol **22:** 1065–1077

Bernacchi CJ, Pimentel C, Long SP (2003) In vivo temperature response functions of parameters required to model RuBP-limited photosynthesis. Plant Cell Environ **26:** 1419–1430

Bernacchi CJ, Portis AR, Nakano H, von Caemmerer S, Long SP (2002) Temperature response of mesophyll conductance. Implications for the determination of Rubisco enzyme kinetics and for limitations to photosynthesis in vivo. Plant Physiol **130:** 1992–1998

Bernacchi CJ, Singsaas EL, Pimentel C, Portis AR, Long SP (2001) Improved temperature response functions for models of Rubisco-limited photosynthesis. Plant Cell Environ **24:** 253–259

Bradford, M (1976) A rapid and sensitive method for the quantification of microgram quantities of protein utilizing the principle of protein-dye binding. Analytical Biochemistry **72:** 248–254

Campbell BW, Mani D, Curtin SJ, Slattery RA, Michno J-M, Ort DR, Schaus PJ, Palmer RG, Orf JH, Stupar RM (2015) Identical substitutions in magnesium chelatase paralogs result in chlorophyll-deficient soybean mutants. G3 **5:** 123–131

Campbell G, Norman J (1998) Introduction to Environmental Biophysics. Springer, Berlin, Germany

Del Pozo A, Dennett MD (1999) Analysis of the distribution of light, leaf nitrogen, and photosynthesis within the canopy of *Vicia faba* L. at two contrasting plant densities. Aust J Agric Res **50:** 183–190

De Pury D, Farquhar GD (1997) Simple scaling of photosynthesis from leaves to canopies without the errors of big-leaf models. Plant Cell Environ **20:** 537–557

Dornhoff GM, Shibles R (1976) Leaf morphology and anatomy in relation to CO_2-exchange rate of soybean leaves. Crop Sci **16:** 377–381

Dreccer MF, van Oijen M, Schapendonk AHCM, Pot CS, Rabbinge R (2000) Dynamics of vertical leaf nitrogen distribution in a vegetative wheat canopy. Impact on canopy photosynthesis. Ann Bot (Lond) **86:** 821–831

Drewry DT, Kumar P, Long SP (2014) Simultaneous improvement in productivity, water use, and albedo through crop structural modification. Glob Change Biol **20:** 1955–1967

Drewry DT, Kumar P, Long S, Bernacchi C, Liang XZ, Sivapalan M (2010a) Ecohydrological responses of dense canopies to environmental

variability: 1. Interplay between vertical structure and photosynthetic pathway. J Geophys Res Biogeosci **115:** G04022

Drewry DT, Kumar P, Long S, Bernacchi C, Liang XZ, Sivapalan MCG (2010b) Ecohydrological responses of dense canopies to environmental variability: 2. Role of acclimation under elevated CO_2. J Geophys Res Biogeosci **115:** G04023

Evans JR, Poorter H (2001) Photosynthetic acclimation of plants to growth irradiance: the relative importance of specific leaf area and nitrogen partitioning in maximizing carbon gain. Plant Cell Environ **24:** 755–767

Evans JR, Seemann JR (1989) The allocation of protein nitrogen in the photosynthetic apparatus: costs, consequences, and control. Photosynthesis 183–205

Evans JR, von Caemmerer S (1996) Carbon dioxide diffusion inside leaves. Plant Physiol **110:** 339–346

Farquhar GD, Sharkey TD (1982) Stomatal conductance and photosynthesis. Annu Rev Plant Physiol **33:** 317–345

Field C (1983) Allocating leaf nitrogen for the maximization of carbon gain: Leaf age as a control on the allocation program. Oecologia **56:** 341–347

Flexas J, Ortuño MF, Ribas-Carbo M, Diaz-Espejo A, Flórez-Sarasa ID, Medrano H (2007) Mesophyll conductance to CO_2 in *Arabidopsis thaliana*. New Phytol **175:** 501–511

Foyer CH, Shigeoka S (2011) Understanding oxidative stress and antioxidant functions to enhance photosynthesis. Plant Physiol **155:** 93–100

González-Bayón R, Kinsman EA, Quesada V, Vera A, Robles P, Ponce MR, Pyke KA, Micol JL (2006) Mutations in the RETICULATA gene dramatically alter internal architecture but have little effect on overall organ shape in Arabidopsis leaves. J Exp Bot **57:** 3019–3031

Goudriaan J (1977) Crop Micrometeorology: a Simulation Study. Pudoc, Wageningen, Germany

Gu J, Zhou Z, Li Z, Chen Y, Wang Z, Zhang H (2017a) Rice (*Oryza sativa* L.) with reduced chlorophyll content exhibit higher photosynthetic rate and efficiency, improved canopy light distribution, and greater yields than normally pigmented plants. Field Crops Res **200:** 58–70

Gu J, Zhou Z, Li Z, Chen Y, Wang Z, Zhang H, Yang J (2017b) Photosynthetic properties and potentials for improvement of photosynthesis in pale green leaf rice under high light conditions. Front Plant Sci **8:** 108210.3389/fpls.2017.01082. eCollection 2017

Gutschick V (1988) Optimization of specific leaf mass, internal CO_2 concentration, and chlorophyll content in crop canopies. Plant Physiol Biochem **26:** 525–537

Gutschick V (1984a) Photosynthesis model for C_3 leaves incorporating CO_2 transport, radiation propagation, and biochemistry. 1. Kinetics and their parametrization. Photosynthetica **18:** 549–568

Gutschick V (1984b) Photosynthesis model for C_3 leaves incorporating CO_2 transport, radiation propagation, and biochemistry. 2. Ecological and agricultural utility. Photosynthetica **18:** 569–595

Hikosaka K, Niinemets U, Anten NP (2016) Canopy Photosynthesis: from Basics to Applications. Springer, Berlin, Germany

Hikosaka K, Terashima I (1995) A model of the acclimation of photosynthesis in the leaves of C_3 plants to sun and shade with respect to nitrogen use. Plant Cell Environ **18:** 605–618

Houborg R, Cescatti A, Migliavacca M, Kustas WP (2013) Satellite retrievals of leaf chlorophyll and photosynthetic capacity for improved modeling of GPP. Agric For Meteorol **177:** 10–23

Kirst H, Gabilly ST, Niyogi KK, Lemaux PG, Melis A (2017) Photosynthetic antenna engineering to improve crop yields. Planta **245:** 1009–1020

Kirst H, Garcia-Cerdan JG, Zurbriggen A, Ruehle T, Melis A (2012) Truncated photosystem chlorophyll antenna size in the green microalga *Chlamydomonas reinhardtii* upon deletion of the TLA3-CpSRP43 gene. Plant Physiol **160:** 2251–2260

Koester RP, Skoneczka JA, Cary TR, Diers BW, Ainsworth EA (2014) Historical gains in soybean (*Glycine max* Merr.) seed yield are driven by linear increases in light interception, energy conversion, and partitioning efficiencies. J Exp Bot **65:** 3311–3321

Kromdijk J, Long SP (2016) One crop breeding cycle from starvation? How engineering crop photosynthesis for rising CO2 and temperature could be one important route to alleviation. Proc Roy Soc B Biol Sci **283:** 20152578

Kühlbrandt W, Wang DN, Fujiyoshi Y (1994) Atomic model of plant light-harvesting complex by electron crystallography. Nature **367:** 614–621

Lai C-T, Katul G, Oren R, Ellsworth D, Schäfer K (2000) Modeling CO_2 and water vapor turbulent flux distributions within a forest canopy. J Geophys Res D Atmospheres **105:** 26333–26351

Laisk A (1982) Correspondence of photosynthetic system to environmental conditions. *In* Fiziologiya Fotosinteza, Nauka, Moscow, Russia, pp 221–234

Lange BM, Ghassemian M (2003) Genome organization in *Arabidopsis thaliana*: a survey for genes involved in isoprenoid and chlorophyll metabolism. Plant Mol Biol **51:** 925–948

Lee C-G (1999) Calculation of light penetration depth in photobioreactors. Biotechnol Bioprocess Eng **4:** 78–81

Leuning R, Kelliher FM, De Pury DGG, Schulze ED (1995) Leaf nitrogen, photosynthesis, conductance and transpiration: scaling from leaves to canopies. Plant Cell Environ **18:** 1183–1200

Lindgren LO, Stålberg KG, Höglund A-S (2003) Seed-specific overexpression of an endogenous Arabidopsis phytoene synthase gene results in delayed germination and increased levels of carotenoids, chlorophyll, and abscisic acid. Plant Physiol **132:** 779–785

Long SP, Marshall-Colon A, Zhu X-G (2015) Meeting the global food demand of the future by engineering crop photosynthesis and yield potential. Cell **161:** 56–66

Long SP, Zhu X-G, Naidu SL, Ort DR (2006) Can improvement in photosynthesis increase crop yields? Plant Cell Environ **29:** 315–330

Melis A (1999) Photosystem-II damage and repair cycle in chloroplasts: what modulates the rate of photodamage? Trends Plant Sci **4:** 130–135

Mitra M, Melis A (2008) Optical properties of microalgae for enhanced biofuels production. Opt Express **16:** 21807–21820

Moreau D, Allard V, Gaju O, Le Gouis J, Foulkes MJ, Martre P (2012) Acclimation of leaf nitrogen to vertical light gradient at anthesis in wheat is a whole-plant process that scales with the size of the canopy. Plant Physiol **160:** 1479–1490

Netto AT, Campostrini E, Oliveira JGE, Bressan-Smith RE (2005) Photosynthetic pigments, nitrogen, chlorophyll a fluorescence and SPAD-502 readings in coffee leaves. Sci Hortic (Amsterdam) **104:** 199–209

Niinemets U (2007) Photosynthesis and resource distribution through plant canopies. Plant Cell Environ **30:** 1052–1071

Niinemets Ü, Keenan TF, Hallik L (2015) A worldwide analysis of within-canopy variations in leaf structural, chemical and physiological traits across plant functional types. New Phytol **205:** 973–993

Niinemets Ü, Tenhunen JD (1997) A model separating leaf structural and physiological effects on carbon gain along light gradients for the shade-tolerant species *Acer saccharum*. Plant Cell Environ **20:** 845–866

Ort DR (2001) When there is too much light. Plant Physiol **125:** 29–32

Ort DR, Melis A (2011) Optimizing antenna size to maximize photosynthetic efficiency. Plant Physiol **155:** 79–85

Ort DR, Merchant SS, Alric J, Barkan A, Blankenship RE, Bock R, Croce R, Hanson MR, Hibberd JM, Long SP, Moore TA, Moroney J, et al (2015) Redesigning photosynthesis to sustainably meet global food and bioenergy demand. Proc Natl Acad Sci USA **112:** 8529–8536

Osborne BA, Raven JA (1986) Light absorption by plants and its implications for photosynthesis. Biol Rev Camb Philos Soc **61:** 1–60

Paltineanu IC, Starr JL (1997) Real-time soil water dynamics using multisensor capacitance probes: laboratory calibration. Soil Sci Soc Am J **61:** 1576–1585

Pettigrew WT, Hesketh JD, Peters DB, Woolley JT (1989) Characterization of canopy photosynthesis of chlorophyll-deficient soybean isolines. Crop Sci **29:** 315–330

Polle JEW, Kanakagiri SD, Melis A (2003) tla1, a DNA insertional transformant of the green alga *Chlamydomonas reinhardtii* with a truncated light-harvesting chlorophyll antenna size. Planta **217:** 49–59

Ray DK, Mueller ND, West PC, Foley JA (2013) Yield trends are insufficient to double global crop production by 2050. PLoS One **8:** e66428

Ritchie RJ (2006) Consistent sets of spectrophotometric chlorophyll equations for acetone, methanol and ethanol solvents. Photosynth Res **89:** 27–41

Salvagiotti F, Cassman KG, Specht JE, Walters DT, Weiss A, Dobermann A (2008) Nitrogen uptake, fixation and response to fertilizer N in soybeans: a review. Field Crops Res **108:** 1–13

Sands P (1995) Modelling canopy production. I. Optimal distribution of photosynthetic resources. Funct Plant Biol **22:** 593–601

Schieving F, Pons TL, Werger MJA, Hirose T (1992) The vertical distribution of nitrogen and photosynthetic activity at different plant densities in *Carex acutiformis*. Plant Soil **142:** 9–17

Sharkey TD, Bernacchi CJ, Farquhar GD, Singsaas EL (2007) Fitting photosynthetic carbon dioxide response curves for C_3 leaves. Plant Cell Environ **30:** 1035–1040

Slattery RA, Grennan AK, Sivaguru M, Sozzani R, Ort DR (2016) Light sheet microscopy reveals more gradual light attenuation in light-green versus dark-green soybean leaves. J Exp Bot **67:** 4697–4709

Slattery RA, Ort DR (2015) Photosynthetic energy conversion efficiency: setting a baseline for gauging future improvements in important food and biofuel crops. Plant Physiol **168:** 383–392

Slattery RA, VanLoocke A, Bernacchi CJ, Zhu XG, Ort DR (2017) Photosynthesis, light use efficiency, and yield of reduced-chlorophyll soybean mutants in field conditions. Front Plant Sci **8:** 549

Song Q, Wang Y, Qu M, Ort DR, Zhu X The impact of modifying antenna size of photosystem II on canopy photosynthetic efficiency. Plant Cell Environ **40:** 2946–2957

Spinrad RW, Brown JF (1986) Relative real refractive index of marine microorganisms: a technique for flow cytometric estimation. Appl Opt **25:** 1930–1934

Syvertsen JP, Lloyd J, McConchie C, Kriedemann PE, Farquhar GD (1995) On the relationship between leaf anatomy and CO_2 diffusion through the mesophyll of hypostomatous leaves. Plant Cell Environ **18:** 149–157

Telfer A, Pascal A, Gall A (2008) Carotenoids in photosynthesis. *In* G Britton, S Liaaen-Jensen, H Pfander, eds, Carotenoids, **Volume 4: Natural Functions**. Birkhäuser, Basel, Switzerland, pp 265–308

Terashima I, Saeki T (1983) Light environment within a leaf I. Optical properties of paradermal sections of camellia leaves with special reference to differences in the optical properties of palisade and spongy tissues. Plant Cell Physiol **24:** 1493–1501

Vass I, Cser K (2009) Janus-faced charge recombinations in photosystem II photoinhibition. Trends Plant Sci **14:** 200–205

Woolley JT (1971) Reflectance and transmittance of light by leaves. Plant Physiol **47:** 656–662

Xu D, Chen X, Zhang L, Wang R, Hesketh J (1994) Leaf photosynthesis and chlorophyll fluorescence in a chlorophyll-deficient soybean mutant. Photosynthetica **29:** 103–112

Yin X, Lantinga EA, Schapendonk AHCM, Zhong X (2003) Some quantitative relationships between leaf area index and canopy nitrogen content and distribution. Ann Bot **91:** 893–903

Zhu X-G, de Sturler E, Long SP (2007) Optimizing the distribution of resources between enzymes of carbon metabolism can dramatically increase photosynthetic rate: a numerical simulation using an evolutionary algorithm. Plant Physiol **145:** 513–526

Zhu X-G, Long SP, Ort DR (2008) What is the maximum efficiency with which photosynthesis can convert solar energy into biomass? Curr Opin Biotechnol **19:** 153–159